



Research article

Impacts of magnetic field and thermal radiation on squeezing flow and heat transfer of third grade nanofluid between two disks embedded in a porous medium

M.G. Sobamowo^{*}, A.A. Yinusa, S.T. Aladenusi*Department of Mechanical Engineering, University of Lagos, Akoka, Lagos, Nigeria*

ARTICLE INFO

Keywords:

Applied mathematics
 Computational mathematics
 Mechanical engineering
 Thermal radiation
 Third-grade nanofluid
 Squeezing flow
 Magnetohydrodynamic
 Differential transformation method

ABSTRACT

In this present study, the impacts of magnetic field and thermal radiation on squeezing flow and heat transfer of third grade nanofluid between two disks embedded in a porous medium with temperature jump boundary conditions is analyzed using differential transformation method. The results of the approximate analytical solutions are verified using a fifth-order Runge-Kutta Fehlberg method (Cash-Karp Runge-Kutta) coupled with shooting method. From the analysis, the results of the two methods show excellent agreements. Also, the parametric studies using the approximate analytical solutions show that for a suction parameter greater than zero, the radial velocity of the lower disc increases while that of the upper disc decreases as a result of a corresponding increase in the viscosity of the fluid from the lower squeezing disc to the upper disc. For an increasing magnetic field parameter, the radial velocity of the lower disc decreases while that of the upper disc increases. As the third grade fluid parameter increases, there is a reduction in the fluid viscosity thereby increasing resistance between the fluid molecules. Also, it is found that as the radiation parameter increases, rate of heat transfer to the third grade fluid increases. There is a recorded decrease in the fluid temperature profile as the Prandtl number increases due to decrease in the thermal diffusivity of the third grade fluid. The agreement of the results of the present study and the experimental work shows the validation of the models used in this work to study the flow behaviour of the fluid. It is envisaged that the present work will increase the understanding of the flow behaviour of third grade nanofluid and heat transfer processes as evident in coal slurries, polymer solutions, textiles, ceramics, catalytic reactors, oil recovery applications etc.

1. Introduction

The various applications of non-Newtonian fluids such as in catalytic reactors, oil recovery applications, power transmission, nasogastric tubes, hydraulic lifts, electric motors etc. have in recent times continued to arouse the interests of fluid dynamics and thermal engineering researchers. Also, the continuous wide areas of engineering, industrial and biological applications of fluid and heat transfer flow between two parallel discs or surfaces call for renewed studies and analysis the flow and heat transfer problems. In the past few decades, different studies have been presented on flow, heat and mass transfer analyses of non-Newtonian fluid. In such studies, Mustafa et al. [1] presented transient heat transfer analysis of squeezing fluid flow through two parallel surfaces. Hayat et al. [2] examined the flow of a second grade fluid being squeezed by two parallel discs and presented with proper comparison the

behaviour of the second grade fluid considering or neglecting magnetic effect. In an attempt to solve the extension of Hayat et al model considering suction and injection on magneto-hydrodynamic squeezing flow, Domairry and Aziz [3] adopted a semi-analytical method, homotopy perturbation method to obtain a symbolic solution for investigating and predicting the influence of suction and injection on magnetohydrodynamic (MHD) squeezing flow under standard conditions. A similar study was performed by Siddiqui et al. [4] using two parallel plates with the squeezing viscous fluid under transient condition. In the same year, Rashidi et al. [5] approached the problem using different analytical schemes. Incorporating nanotechnology into the problem of squeezing flow, Khan and Aziz [6, 7], investigated on the effect of natural convection on fluids with nanoparticles. In an extended study, the influence of porosity on the squeezing flow of nanofluids was considered. Another study on squeezing nanofluid flow between two vertical plates was

^{*} Corresponding author.E-mail address: mikegbeminiyiprof@yahoo.com (M.G. Sobamowo).

performed by Kuznestov and Nield [8]. The authors investigated the boundary layer of the squeezing process by using natural convection principle of fluid flow to generate different governing models. Hashimi et al. [9] utilized the models and obtained analytical solutions to the governing equations with the assumption of no slip and no temperature jump in the solid-liquid interface. Although, there some other studies presented on the magnetohydrodynamics flow of nanofluids [10, 11, 12, 13, 14], these studies are based on the assumption of no slip and no temperature jump. However, the two annulled assumptions have to a reasonable extent influence on the flow and heat transfer processes in under investigation. In other to provide an extension to the works of the previous studies by considering slip condition, an appreciable number of studies have been presented on squeezable fluids of different nano-particles sizes, different concentration, different stretching effect and different phases by taking slip into account [15, 16, 17, 18].

Past research works have presented magnetohydrodynamic fluid flow considering porous medium, nanofluid and some other factors capable of reshaping the squeezing process from idealization into reality [19, 20, 21, 22, 23, 24, 25, 26, 27, 28, 29, 30, 31, 32, 33, 34, 35, 36, 37, 38, 39, 40, 41, 42, 43, 44, 45, 46, 47, 48, 49, 50, 51, 52, 53, 54, 55, 56, 57, 58, 59, 60]. Flow analyses of third grade fluids such as slurry flows, dilute polymer solution (polyisobutane, methylmethacrylate in n-butyl acetate), molten plastics, food rheology polymers mixed with melts, manufacturing oils and polymer melts like high viscosity silicon oils, blood, etc. have been subjects of great interests to various fluid mechanics researchers. Therefore, in recent times, the flow and heat transfer characteristics of third grade nanofluid in pipes and channels have been analyzed [61, 62, 63]. Following the findings of Fosdick and Rajagopal [64] that third grade fluid gives different properties to those of fluids such as Newtonian and second grade fluids, Majhi and Nair [65] examined the shearing stresses at the wall of a fluid flow process considering a third grade fluid as the working fluid. The authors compared their obtained results to the results of numerical methods in the work of Masoudi and Christie [66] and an excellent agreement was reached by the two sets of results. In another work, a third grade fluid with constant viscosity was analyzed by Yurusoy and Pakdemirli [67]. The authors developed approximate analytical solutions and verify their work with the numerical solution of the work of Vajrevelu et al. [68]. The research work gave interesting results and found great application in rotary devices. Other studies on third grade fluids includes the fluctuating fluid flow by Hayat et al. [69], boundary layer analysis by Muhammet [70], heat transfer analysis by Yurusoy [71], entropy generation analysis by Pakdemirli et al. [72] and partial slip analysis by Sajid et al. [73]. Different schemes have also been employed to efficiently solve the resulting ordinary differential equations associated with squeezing fluid flow between two parallel surfaces as presented by [74, 75, 76, 77, 78, 79, 80]. In very recent study, Hayat et al. [81] utilized homotopy analysis method analyze the axisymmetric squeezing flow and heat transfer of third grade nanofluid under convective conditions. However, to the best of our knowledge, the study of magnetohydrodynamic unsteady squeezing flow of third grade nanofluid between two parallel disks embedded in a porous medium under the influences of thermal radiation and temperature jump condition using differential transformation method (DTM) has not been considered and analyzed in literature. Therefore, in this work, differential transformation method is applied to carry out nonlinear analysis of unsteady squeezing flow and heat transfer of a third grade nanofluid between two parallel disks embedded in a porous medium under the influences of thermal radiation and magnetic field with temperature-jump boundary conditions. The method as applied in the equation converges very fast and is very efficient for the handling of both ordinary and partial differential equations. In order to verify the approximate analytical solution, a fifth-order Runge-Kutta Fehlberg method (Cash-Karp Runge-Kutta) coupled with shooting method is used. The results of the two methods show excellent agreements. Also, the influences of various parameters on the flow and heat transfer processes are studied and discussed.

2. Problem formulation

Consider an unsteady axisymmetrically flow of third grade nanofluid through two parallel disks as shown in Figure 1. As presented in the Figure, the upper disk is moving towards a stationary lower disk subjected to a uniform magnetic field strength applied perpendicular to the disks. It is assumed that the disks are maintained at constant temperature while the fluid structure is everywhere in thermodynamic equilibrium.

For an incompressible homogeneous thermodynamically compatible third grade fluid, the Cauchy stress tensor, τ is given by

$$\tau = p\mathbf{I} + \mu\mathbf{A}_1 + \alpha_1\mathbf{A}_2 + \alpha_2\mathbf{A}_1^2 + \beta_1\mathbf{A}_3 + \beta_2(\mathbf{A}_1\mathbf{A}_2 + \mathbf{A}_2\mathbf{A}_1) + \beta_3(\text{tr}\mathbf{A}_1^2)\mathbf{A}_1. \quad (1)$$

This Rivlin Ericksen tensor ($\mathbf{A}_1, \mathbf{A}_2$ and \mathbf{A}_3) is a temporal evolution of strain rate tensor such that the derivative rotate and translate with the flow field and can be derived from

$$\mathbf{A}_1 = (\text{grad } \mathbf{V}) + (\text{grad } \mathbf{V})^T, \quad (2)$$

$$\mathbf{A}_n = \frac{d\mathbf{A}_{n-1}}{dt} + \mathbf{A}_{n-1}(\text{grad } \mathbf{V}) + (\text{grad } \mathbf{V})^T\mathbf{A}_{n-1}, \quad n \geq 1 \quad (3)$$

For the motions of the fluid, Clausius-Duhem inequality must be satisfied [64]. The conditions that fluid motions are thermodynamically compatible, the Clausius-Duhem inequality is satisfied and the assumption that the Helmholtz free energy is minimum when the fluid is locally at rest (stable) are given as

$$\mu \geq 0, \alpha_1 \geq 0, \beta_1 = \beta_2 = 0, \beta_3 \geq 0, |\alpha_1 + \alpha_2| \leq \sqrt{24\mu\beta_3}, \quad \beta_1 = \beta_2 = 0, \quad \beta \geq 0 \quad (4)$$

The equation for the velocity and temperature fields are given as

$$\mathbf{V} = (\bar{u}(t, r, z), 0, \bar{w}(t, r, z)) \text{ and } \mathbf{T} = \bar{T}(t, r, z) \quad (5)$$

Using Eqs. (1), (2), (3), (4), and (5), the algebraic forms of the conservation equations can be developed as;

$$\frac{\partial \bar{u}}{\partial r} + \frac{\bar{u}}{r} + \frac{\partial \bar{w}}{\partial z} = 0 \quad (6)$$

$$\rho_{nf} \left(\frac{\partial \bar{u}}{\partial t} + \bar{u} \frac{\partial \bar{u}}{\partial r} + \bar{w} \frac{\partial \bar{u}}{\partial z} \right) = \frac{\partial \tau_{rr}}{\partial r} + \frac{\partial \tau_{rz}}{\partial z} + \frac{\tau_{rr} - \tau_{\theta\theta}}{r} - \frac{\sigma_{nf} B_0^2 \bar{u}}{1 - ct} - \frac{\mu_{nf} \bar{u}}{K} \quad (7)$$

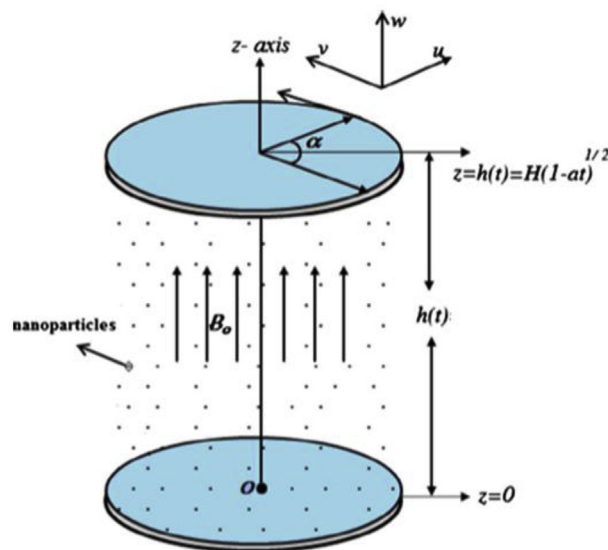


Figure 1. The squeezing flow of Third grade nanofluid between parallel circular plate.

$$\rho_{nf} \left(\frac{\partial \bar{w}}{\partial t} + \bar{u} \frac{\partial \bar{w}}{\partial r} + \bar{w} \frac{\partial \bar{w}}{\partial z} \right) = \frac{1}{r} \frac{\partial}{\partial r} (r \tau_{rr}) + \frac{\partial \tau_{rz}}{\partial z} - \frac{\mu_{nf}}{K} \bar{w} \tag{8}$$

where

$$\begin{aligned} \tau_{rr} = & -p + 2\mu_{nf} \frac{\partial \bar{u}}{\partial r} + 2(\alpha_1)_{nf} \left[\bar{u} \frac{\partial^2 \bar{u}}{\partial r^2} + \bar{w} \frac{\partial^2 \bar{u}}{\partial r \partial z} + 2 \left(\frac{\partial \bar{u}}{\partial r} \right)^2 + \frac{\partial \bar{w}}{\partial r} \left(\frac{\partial \bar{u}}{\partial z} + \frac{\partial \bar{w}}{\partial r} \right) \right] \\ & + (\alpha_2)_{nf} \left[4 \left(\frac{\partial \bar{u}}{\partial r} \right)^2 + \left(\frac{\partial \bar{u}}{\partial z} + \frac{\partial \bar{w}}{\partial r} \right)^2 \right] + 4(\beta_3)_{nf} \frac{\partial \bar{u}}{\partial r} \left[2 \frac{\bar{u}^2}{r^2} + \left(\frac{\partial \bar{u}}{\partial z} + \frac{\partial \bar{w}}{\partial r} \right)^2 \right] \\ & + \left\{ 2 \left(\frac{\partial \bar{u}}{\partial r} \right)^2 + \left(\frac{\partial \bar{w}}{\partial z} \right)^2 \right\} \end{aligned} \tag{9}$$

$$\begin{aligned} \tau_{\theta\theta} = & -p + 2\mu_{nf} \frac{\bar{u}}{r} + 2(\alpha_1)_{nf} \left[\bar{u} \frac{\partial \bar{u}}{\partial r} + \bar{w} \frac{\partial \bar{u}}{\partial z} + \frac{\bar{u}^2}{r^2} \right] + 4(\alpha_2)_{nf} \frac{\bar{u}^2}{r^2} \\ & + 4(\beta_3)_{nf} \frac{\bar{u}}{r} \left[2 \frac{\bar{u}^2}{r^2} + \left(\frac{\partial \bar{u}}{\partial z} + \frac{\partial \bar{w}}{\partial r} \right)^2 + \left\{ 2 \left(\frac{\partial \bar{u}}{\partial r} \right)^2 + \left(\frac{\partial \bar{w}}{\partial r} \right)^2 \right\} \right] \end{aligned} \tag{10}$$

$$\tau_{zz} = -p + 2\mu_{nf} \frac{\partial \bar{w}}{\partial z} + 2(\alpha_1)_{nf} \left[\bar{u} \frac{\partial^2 \bar{w}}{\partial r \partial z} + \bar{w} \frac{\partial^2 \bar{w}}{\partial z^2} + 2 \left(\frac{\partial \bar{w}}{\partial r} \right)^2 + \frac{\partial \bar{u}}{\partial z} \left(\frac{\partial \bar{u}}{\partial z} + \frac{\partial \bar{w}}{\partial r} \right) \right]$$

$$\begin{aligned} & + (\alpha_2)_{nf} \left[4 \left(\frac{\partial \bar{w}}{\partial r} \right)^2 + \left(\frac{\partial \bar{u}}{\partial z} + \frac{\partial \bar{w}}{\partial r} \right)^2 \right] + 4(\beta_3)_{nf} \left(\frac{\partial \bar{w}}{\partial z} \right) \left[2 \frac{\bar{u}^2}{r^2} + \left(\frac{\partial \bar{u}}{\partial z} + \frac{\partial \bar{w}}{\partial r} \right)^2 \right] \\ & + \left\{ 2 \left(\frac{\partial \bar{u}}{\partial r} \right)^2 + \left(\frac{\partial \bar{w}}{\partial z} \right)^2 \right\} \end{aligned} \tag{11}$$

$$\begin{aligned} \tau_{rz} = & \mu_{nf} \left(\frac{\partial \bar{u}}{\partial z} + \frac{\partial \bar{w}}{\partial r} \right) + (\alpha_1)_{nf} \left[\left(\bar{u} \frac{\partial}{\partial r} + \bar{w} \frac{\partial}{\partial z} \right) \left(\frac{\partial \bar{u}}{\partial z} + \frac{\partial \bar{w}}{\partial r} \right) + \frac{\partial \bar{u}}{\partial r} \frac{\partial \bar{w}}{\partial r} \right. \\ & + \frac{\partial \bar{u}}{\partial z} \frac{\partial \bar{w}}{\partial z} + 3 \left(\frac{\partial \bar{u}}{\partial r} \frac{\partial \bar{u}}{\partial z} + \frac{\partial \bar{w}}{\partial r} \frac{\partial \bar{w}}{\partial z} \right) \left. \right] + 2(\alpha_2)_{nf} \left(\frac{\partial \bar{u}}{\partial r} + \frac{\partial \bar{w}}{\partial z} \right) \left(\frac{\partial \bar{u}}{\partial z} + \frac{\partial \bar{w}}{\partial r} \right) \\ & + 2(\beta_3)_{nf} \left(\frac{\partial \bar{u}}{\partial z} + \frac{\partial \bar{w}}{\partial r} \right) \left[2 \frac{\bar{u}^2}{r^2} + \left(\frac{\partial \bar{u}}{\partial z} + \frac{\partial \bar{w}}{\partial r} \right)^2 + \left\{ 2 \left(\frac{\partial \bar{u}}{\partial r} \right)^2 + \left(\frac{\partial \bar{w}}{\partial z} \right)^2 \right\} \right] \end{aligned} \tag{12}$$

After substitution of Eqs. (9), (10), (11), and (12) into above momentum equations in Eqs. (7) and (8) and expansion of the resulting equations, one arrives at Eqs. (13) and (14)

$$\begin{aligned} \rho_{nf} \left(\frac{\partial \bar{u}}{\partial t} + \bar{u} \frac{\partial \bar{u}}{\partial r} + \bar{w} \frac{\partial \bar{u}}{\partial z} \right) = & -\frac{\partial p}{\partial r} + \mu \left(\frac{\partial^2 \bar{u}}{\partial r^2} + \frac{\partial^2 \bar{u}}{\partial z^2} + \frac{1}{r} \frac{\partial \bar{u}}{\partial r} - \frac{\bar{u}}{r^2} \right) + \\ & \left[\begin{aligned} & -2 \frac{\bar{u}^2}{r^3} - \frac{2}{r^2} \frac{\partial \bar{u}}{\partial t} + \frac{4}{r} \left(\frac{\partial \bar{u}}{\partial r} \right)^2 + 3 \frac{\partial \bar{u}}{\partial r} \frac{\partial^2 \bar{u}}{\partial z^2} + 5 \frac{\partial \bar{w}}{\partial r} \frac{\partial^2 \bar{u}}{\partial r \partial z} + 3 \frac{\partial \bar{u}}{\partial z} \frac{\partial^2 \bar{w}}{\partial r^2} + 2 \frac{\bar{w}}{r} \frac{\partial^2 \bar{u}}{\partial r \partial z} + \frac{2}{r} \left(\frac{\partial \bar{w}}{\partial r} \right)^2 \\ & -2 \frac{\bar{u}}{r^2} \frac{\partial \bar{u}}{\partial r} + 4 \frac{\partial \bar{w}}{\partial z} \frac{\partial^2 \bar{w}}{\partial r \partial z} + \frac{\partial \bar{u}}{\partial r} \frac{\partial^2 \bar{w}}{\partial r \partial z} + 2 \frac{\partial \bar{w}}{\partial z} \frac{\partial^2 \bar{u}}{\partial z^2} + \bar{u} \frac{\partial^3 \bar{u}}{\partial r \partial z^2} + \bar{w} \frac{\partial^3 \bar{w}}{\partial r \partial z^2} + 3 \frac{\partial \bar{w}}{\partial r} \frac{\partial^2 \bar{w}}{\partial z^2} \\ & -2 \frac{\bar{w}}{r^2} \frac{\partial \bar{u}}{\partial z} + \frac{\partial^3 \bar{u}}{\partial z^2 \partial t} + \bar{w} \frac{\partial^3 \bar{u}}{\partial z^3} + 4 \frac{\partial \bar{w}}{\partial r} \frac{\partial^2 \bar{w}}{\partial r^2} + 2 \bar{w} \frac{\partial^3 \bar{u}}{\partial r^2 \partial z} + \frac{2}{r} \frac{\partial \bar{u}}{\partial z} \frac{\partial \bar{w}}{\partial r} + 4 \frac{\partial \bar{u}}{\partial z} \frac{\partial^2 \bar{u}}{\partial r \partial z} \\ & + 10 \frac{\partial \bar{u}}{\partial r} \frac{\partial^2 \bar{u}}{\partial r^2} + \frac{2}{r} \frac{\partial^2 \bar{u}}{\partial r \partial t} + \frac{\partial^3 \bar{w}}{\partial r \partial z \partial t} + \bar{u} \frac{\partial^3 \bar{u}}{\partial r^2 \partial z} + 2 \frac{\partial^3 \bar{u}}{\partial r^2 \partial t} + 2 \mu \frac{\partial^3 \bar{u}}{\partial r^3} + 2 \frac{\bar{u}}{r} \frac{\partial^2 \bar{u}}{\partial r^2} + \frac{\partial \bar{u}}{\partial z} \frac{\partial^2 \bar{w}}{\partial z^2} \end{aligned} \right] \\ & + (\alpha_2)_{nf} \left[\begin{aligned} & -4 \frac{\bar{u}^2}{r^3} + \frac{4}{r} \left(\frac{\partial \bar{u}}{\partial r} \right)^2 + 2 \frac{\partial \bar{u}}{\partial z} \frac{\partial^2 \bar{w}}{\partial z^2} + 2 \frac{\partial \bar{u}}{\partial r} \frac{\partial^2 \bar{u}}{\partial z^2} + 2 \frac{\partial \bar{w}}{\partial r} \frac{\partial^2 \bar{w}}{\partial z^2} + 4 \frac{\partial \bar{w}}{\partial r} \frac{\partial^2 \bar{u}}{\partial r \partial z} + \frac{1}{r} \left(\frac{\partial \bar{w}}{\partial r} \right)^2 + \frac{1}{r} \left(\frac{\partial \bar{u}}{\partial z} \right)^2 + 8 \frac{\partial \bar{u}}{\partial r} \frac{\partial^2 \bar{u}}{\partial r^2} \\ & + 2 \frac{\partial^2 \bar{w}}{\partial r \partial z} \frac{\partial \bar{w}}{\partial z} + 2 \frac{\partial \bar{u}}{\partial z} \frac{\partial^2 \bar{u}}{\partial r \partial z} + 2 \frac{\partial \bar{w}}{\partial r} \frac{\partial^2 \bar{w}}{\partial r^2} + 2 \frac{\partial \bar{u}}{\partial z} \frac{\partial^2 \bar{w}}{\partial r^2} + 2 \frac{\partial \bar{u}}{\partial r} \frac{\partial^2 \bar{w}}{\partial r \partial z} + \frac{2}{r} \frac{\partial \bar{u}}{\partial z} \frac{\partial \bar{w}}{\partial r} + 2 \frac{\partial \bar{w}}{\partial z} \frac{\partial^2 \bar{u}}{\partial z^2} + 2 \frac{\partial \bar{u}}{\partial z} \frac{\partial^2 \bar{u}}{\partial r \partial z} \end{aligned} \right] \\ & + (\beta_3)_{nf} \left[\begin{aligned} & -8 \frac{\bar{u}^3}{r^3} + 8 \frac{\bar{u}^2}{r^2} \frac{\partial^2 \bar{u}}{\partial r^2} + \frac{8}{r} \left(\frac{\partial \bar{u}}{\partial r} \right)^3 + 24 \left(\frac{\partial \bar{u}}{\partial r} \right)^2 \frac{\partial^2 \bar{u}}{\partial r^2} + \frac{4}{r} \frac{\partial \bar{u}}{\partial r} \left(\frac{\partial \bar{u}}{\partial z} \right)^2 + \frac{4}{r} \frac{\partial \bar{u}}{\partial r} \left(\frac{\partial \bar{w}}{\partial r} \right)^2 + \frac{8}{r} \frac{\partial \bar{u}}{\partial r} \frac{\partial \bar{u}}{\partial z} \frac{\partial \bar{u}}{\partial r} \\ & + 16 \frac{\bar{u}}{r^2} \left(\frac{\partial \bar{u}}{\partial r} \right)^2 + \frac{8}{r} \frac{\partial \bar{u}}{\partial r} \left(\frac{\partial \bar{w}}{\partial z} \right)^2 + 8 \frac{\partial \bar{u}}{\partial r} \frac{\partial \bar{w}}{\partial r} \frac{\partial^2 \bar{w}}{\partial r^2} + 8 \left(\frac{\partial \bar{w}}{\partial z} \right)^2 \frac{\partial^2 \bar{u}}{\partial r^2} - 4 \frac{\bar{u}}{r^2} \left(\frac{\partial \bar{w}}{\partial r} \right)^2 + 16 \frac{\partial \bar{u}}{\partial r} \frac{\partial \bar{u}}{\partial z} \frac{\partial^2 \bar{u}}{\partial r \partial z} \\ & + 4 \frac{\bar{u}^2}{r^2} \frac{\partial^2 \bar{w}}{\partial r \partial z} + 8 \frac{\partial^2 \bar{u}}{\partial r^2} \frac{\partial \bar{u}}{\partial z} \frac{\partial \bar{w}}{\partial r} + 8 \frac{\partial \bar{u}}{\partial r} \frac{\partial \bar{w}}{\partial z} \frac{\partial^2 \bar{w}}{\partial r^2} + 4 \left(\frac{\partial \bar{w}}{\partial z} \right)^2 \frac{\partial^2 \bar{w}}{\partial r \partial z} - 8 \frac{\bar{u}}{r^2} \left(\frac{\partial \bar{u}}{\partial r} \right)^2 + 4 \left(\frac{\partial \bar{u}}{\partial r} \right)^2 \frac{\partial^2 \bar{u}}{\partial z^2} \\ & + 4 \left(\frac{\partial \bar{u}}{\partial r} \right)^2 \frac{\partial^2 \bar{w}}{\partial r \partial z} + 4 \frac{\bar{u}^2}{r^2} \frac{\partial^2 \bar{u}}{\partial z^2} + 16 \frac{\partial \bar{u}}{\partial r} \frac{\partial \bar{w}}{\partial z} \frac{\partial^2 \bar{w}}{\partial r \partial z} + 8 \frac{\partial \bar{u}}{\partial z} \frac{\partial \bar{w}}{\partial z} \frac{\partial^2 \bar{w}}{\partial z^2} + 4 \left(\frac{\partial \bar{w}}{\partial z} \right)^2 \frac{\partial^2 \bar{u}}{\partial z^2} + 4 \frac{\bar{u}}{r^2} \left(\frac{\partial \bar{u}}{\partial z} \right)^2 \\ & + 4 \left(\frac{\partial \bar{w}}{\partial r} \right)^2 \frac{\partial^2 \bar{u}}{\partial r^2} + 6 \left(\frac{\partial \bar{u}}{\partial z} \right)^2 \frac{\partial^2 \bar{u}}{\partial z^2} + 8 \frac{\partial \bar{w}}{\partial r} \frac{\partial \bar{w}}{\partial z} \frac{\partial^2 \bar{w}}{\partial z^2} + 6 \left(\frac{\partial \bar{w}}{\partial r} \right)^2 \frac{\partial^2 \bar{u}}{\partial z^2} - 8 \frac{\bar{u}}{r^2} \left(\frac{\partial \bar{w}}{\partial z} \right)^2 + 6 \left(\frac{\partial \bar{w}}{\partial r} \right)^2 \frac{\partial^2 \bar{w}}{\partial r \partial z} \\ & - 8 \frac{\bar{u}^2}{r^3} \frac{\partial \bar{u}}{\partial r} + 6 \left(\frac{\partial \bar{u}}{\partial z} \right)^2 \frac{\partial^2 \bar{w}}{\partial r \partial z} + 16 \frac{\partial \bar{u}}{\partial r} \frac{\partial \bar{w}}{\partial r} \frac{\partial^2 \bar{u}}{\partial r \partial z} + 12 \frac{\partial \bar{u}}{\partial z} \frac{\partial \bar{w}}{\partial r} \frac{\partial^2 \bar{u}}{\partial z^2} + 12 \frac{\partial \bar{u}}{\partial z} \frac{\partial \bar{w}}{\partial r} \frac{\partial^2 \bar{w}}{\partial r \partial z} + 4 \left(\frac{\partial \bar{u}}{\partial z} \right)^2 \frac{\partial^2 \bar{u}}{\partial r^2} \end{aligned} \right] - \frac{\sigma_{nf} B_0^2 \bar{u}}{1 - ct} - \frac{\mu_{nf}}{K} \bar{u} \end{aligned} \tag{13}$$

And the energy equation is given as

$$\begin{aligned}
 (\rho C_p)_{nf} \left(\frac{\partial \bar{T}}{\partial t} + \bar{u} \frac{\partial \bar{T}}{\partial r} + \bar{w} \frac{\partial \bar{T}}{\partial z} \right) &= k \left(\frac{\partial^2 \bar{T}}{\partial r^2} + \frac{1}{r} \frac{\partial \bar{T}}{\partial r} + \frac{\partial^2 \bar{T}}{\partial z^2} \right) + \mu \left[2 \left(\frac{\partial \bar{u}}{\partial r} \right)^2 + 2 \frac{\bar{u}^2}{r^2} + \left(\frac{\partial \bar{u}}{\partial z} \right)^2 + 2 \frac{\partial \bar{u}}{\partial z} \frac{\partial \bar{w}}{\partial r} + 2 \left(\frac{\partial \bar{w}}{\partial z} \right)^2 + \left(\frac{\partial \bar{w}}{\partial r} \right)^2 \right] \\
 + (\alpha_1)_{nf} &\left[2 \frac{\bar{u}^3}{r^3} + 4 \left(\frac{\partial \bar{u}}{\partial r} \right)^3 + 2 \frac{\bar{u}}{r^2} \frac{\partial \bar{u}}{\partial r} + \bar{u} \frac{\partial \bar{u}}{\partial z} \frac{\partial^2 \bar{w}}{\partial r^2} + \bar{w} \frac{\partial \bar{u}}{\partial z} \frac{\partial^2 \bar{w}}{\partial z^2} + \bar{u} \frac{\partial \bar{w}}{\partial r} \frac{\partial^2 \bar{w}}{\partial r^2} + \bar{u} \frac{\partial \bar{u}}{\partial z} \frac{\partial^2 \bar{u}}{\partial r \partial z} + \frac{\partial \bar{u}}{\partial z} \frac{\partial^2 \bar{u}}{\partial z \partial t} + 2 \frac{\bar{u} \bar{w}}{r^2} \frac{\partial \bar{u}}{\partial z} + \bar{u} \frac{\partial \bar{w}}{\partial r} \frac{\partial^2 \bar{u}}{\partial r \partial z} \right. \\
 &+ \frac{\partial \bar{w}}{\partial r} \frac{\partial^2 \bar{u}}{\partial z \partial t} + \bar{w} \frac{\partial \bar{w}}{\partial r} \frac{\partial^2 \bar{u}}{\partial z^2} + 3 \frac{\partial \bar{u}}{\partial r} \left(\frac{\partial \bar{w}}{\partial r} \right)^2 + 4 \left(\frac{\partial \bar{w}}{\partial z} \right)^3 + 3 \left(\frac{\partial \bar{w}}{\partial r} \right)^2 \frac{\partial \bar{w}}{\partial z} + 2 \bar{u} \frac{\partial \bar{w}}{\partial z} \frac{\partial^2 \bar{w}}{\partial r \partial z} + \bar{w} \frac{\partial \bar{w}}{\partial r} \frac{\partial^2 \bar{w}}{\partial r \partial z} + 3 \left(\frac{\partial \bar{u}}{\partial z} \right)^2 \frac{\partial \bar{w}}{\partial z} \\
 &+ 2 \bar{u} \frac{\partial \bar{w}}{\partial z} \frac{\partial^2 \bar{w}}{\partial r \partial z} + \bar{w} \frac{\partial \bar{w}}{\partial r} \frac{\partial^2 \bar{w}}{\partial r \partial z} + 3 \left(\frac{\partial \bar{u}}{\partial z} \right)^2 \frac{\partial \bar{w}}{\partial z} + 3 \frac{\partial \bar{u}}{\partial r} \left(\frac{\partial \bar{u}}{\partial z} \right)^2 + 6 \frac{\partial \bar{u}}{\partial z} \frac{\partial \bar{w}}{\partial r} \frac{\partial \bar{w}}{\partial z} + 2 \frac{\bar{u}^2}{r^2} \frac{\partial \bar{u}}{\partial r} + \bar{w} \frac{\partial \bar{u}}{\partial z} \frac{\partial^2 \bar{w}}{\partial r \partial z} + 2 \frac{\partial \bar{u}}{\partial r} \frac{\partial^2 \bar{u}}{\partial r \partial t} \\
 &+ \frac{\partial \bar{u}}{\partial z} \frac{\partial^2 \bar{w}}{\partial r \partial t} + \frac{\partial \bar{w}}{\partial r} \frac{\partial^2 \bar{w}}{\partial r \partial t} + 6 \frac{\partial \bar{u}}{\partial r} \frac{\partial \bar{u}}{\partial z} \frac{\partial \bar{w}}{\partial r} + 2 \bar{u} \frac{\partial \bar{u}}{\partial r} \frac{\partial^2 \bar{u}}{\partial r^2} + 2 \bar{w} \frac{\partial \bar{w}}{\partial z} \frac{\partial^2 \bar{w}}{\partial z^2} + 2 \bar{w} \frac{\partial \bar{u}}{\partial r} \frac{\partial^2 \bar{u}}{\partial r \partial z} + 2 \frac{\partial \bar{w}}{\partial z} \frac{\partial^2 \bar{w}}{\partial z \partial t} \left. \right] \\
 + (\alpha_2)_{nf} &\left[4 \frac{\bar{u}^3}{r^3} + 3 \frac{\partial \bar{u}}{\partial r} \left(\frac{\partial \bar{u}}{\partial z} \right)^2 + 3 \frac{\partial \bar{u}}{\partial r} \left(\frac{\partial \bar{w}}{\partial r} \right)^2 + 6 \frac{\partial \bar{u}}{\partial r} \frac{\partial \bar{u}}{\partial z} \frac{\partial \bar{w}}{\partial r} + 6 \frac{\partial \bar{u}}{\partial z} \frac{\partial \bar{w}}{\partial r} \frac{\partial \bar{w}}{\partial z} + 4 \left(\frac{\partial \bar{u}}{\partial r} \right)^3 + 3 \left(\frac{\partial \bar{u}}{\partial z} \right)^2 \frac{\partial \bar{w}}{\partial z} + 4 \left(\frac{\partial \bar{w}}{\partial z} \right)^3 + 3 \left(\frac{\partial \bar{w}}{\partial r} \right)^2 \frac{\partial \bar{w}}{\partial z} \right] \\
 + (\beta_3)_{nf} &\left[2 \left(\frac{\partial \bar{w}}{\partial r} \right)^4 + 8 \frac{\bar{u}^4}{r^4} + 8 \left(\frac{\partial \bar{u}}{\partial r} \right)^2 \left(\frac{\partial \bar{u}}{\partial z} \right)^2 + 2 \left(\frac{\partial \bar{u}}{\partial z} \right)^4 + 16 \frac{\bar{u}^2}{r^2} \left(\frac{\partial \bar{u}}{\partial r} \right)^2 + 8 \left(\frac{\partial \bar{u}}{\partial r} \right)^4 + 16 \frac{\bar{u}^2}{r^2} \frac{\partial \bar{u}}{\partial z} \frac{\partial \bar{w}}{\partial r} + 8 \left(\frac{\partial \bar{u}}{\partial z} \right)^3 \frac{\partial \bar{w}}{\partial r} + 8 \frac{\bar{u}^2}{r^2} \left(\frac{\partial \bar{w}}{\partial r} \right)^2 \right. \\
 &+ 8 \frac{\bar{u}^2}{r^2} \left(\frac{\partial \bar{u}}{\partial z} \right)^2 + 8 \frac{\partial \bar{u}}{\partial z} \left(\frac{\partial \bar{w}}{\partial r} \right)^3 + 12 \left(\frac{\partial \bar{u}}{\partial z} \right)^2 \left(\frac{\partial \bar{w}}{\partial r} \right)^2 + 16 \left(\frac{\partial \bar{u}}{\partial r} \right)^2 \left(\frac{\partial \bar{w}}{\partial z} \right)^2 + 8 \left(\frac{\partial \bar{u}}{\partial r} \right)^2 \left(\frac{\partial \bar{w}}{\partial r} \right)^2 + 8 \left(\frac{\partial \bar{w}}{\partial r} \right)^2 \left(\frac{\partial \bar{w}}{\partial z} \right)^2 + 16 \frac{\bar{u}^2}{r^2} \left(\frac{\partial \bar{w}}{\partial z} \right)^2 \\
 &+ 16 \frac{\partial \bar{u}}{\partial z} \frac{\partial \bar{w}}{\partial r} \left(\frac{\partial \bar{w}}{\partial z} \right)^2 + 8 \left(\frac{\partial \bar{u}}{\partial z} \right)^2 \left(\frac{\partial \bar{w}}{\partial z} \right)^2 + 16 \left(\frac{\partial \bar{u}}{\partial r} \right)^2 \frac{\partial \bar{u}}{\partial z} \frac{\partial \bar{w}}{\partial r} + 8 \left(\frac{\partial \bar{w}}{\partial z} \right)^4 \left. \right] \\
 + \frac{16 \sigma_{nf}^* T_h^3}{3(k_1^*)_{nf}} &\left(\frac{\partial^2 \bar{T}}{\partial r^2} + \frac{1}{r} \frac{\partial \bar{T}}{\partial r} + \frac{\partial^2 \bar{T}}{\partial z^2} \right) + \frac{\sigma_{nf} B_0^2 \bar{u}^2}{1 - ct}
 \end{aligned} \tag{15}$$

The related boundary conditions are given as

$$\begin{aligned}
 \bar{u}(r, z, t) = U_w = \frac{ar}{2(1-ct)}, \quad \bar{w}(r, z, t) = -w_0, \quad -k_{nf} \frac{\partial \bar{T}}{\partial z} = H_1(T_f - \bar{T}) \text{ at } z = 0, \\
 \bar{u}(r, z, t) = 0, \quad \bar{w}(r, z, t) = \frac{\partial h}{\partial t} = -\frac{c}{2} \sqrt{\frac{v}{a(1-ct)}}, \quad -k_{nf} \frac{\partial \bar{T}}{\partial z} = H_2(\bar{T} - T_h) \text{ at } z = h(t),
 \end{aligned} \tag{16}$$

where $w_0 > 0$ represents suction.

The physical and thermal properties in Eqs. (7), (8), (9), (10), (11), (12), (13), (14), and (15) are given as

$$\rho_{nf} = \rho_s \varphi + \rho_f (1 - \varphi) \tag{17}$$

$$(\rho C_p)_{nf} = (\rho C_p)_s \varphi + (\rho C_p)_f (1 - \varphi) \tag{18}$$

$$(\rho \beta)_{nf} = (\rho \beta)_s \varphi + (\rho \beta)_f (1 - \varphi) \tag{19}$$

$$\mu_{nf} = \mu_f (1 - \varphi)^{-2.5} \tag{20}$$

$$\sigma_{nf} = \sigma_f \left[1 + \left\{ 3 \left\{ \frac{\sigma_s}{\sigma_f} - 1 \right\} \varphi \left\{ \left\{ \frac{\sigma_s}{\sigma_f} + 2 \right\} \varphi - \left\{ \frac{\sigma_s}{\sigma_f} - 1 \right\} \varphi \right\}^{-1} \right\} \right], \tag{21}$$

$$k_{nf} = k_f [k_s + 2k_f - 2\varphi(k_f - k_s)] [k_s + 2k_f + \varphi(k_f - k_s)]^{-1} \tag{22}$$

$$\frac{\partial q_r}{\partial y} = -\frac{4\sigma}{3K} \frac{\partial \bar{T}^4}{\partial y} \cong -\frac{16\sigma T_s^3}{3K} \frac{\partial^2 \bar{T}}{\partial y^2} \text{ (using Rosseland's approximation)} \tag{23}$$

The nanofluid in this present study contains pure water as the base fluid while Copper (II) Oxide (CuO) as the nanoparticles. Tables 1 and 2 present the physical and thermal properties of the base fluid and the nanoparticles, respectively.

Using the following similarity variables for the transformations of the system of partial differential equations to system of ordinary differential equations:

$$\eta = \frac{z}{h(t)}, \quad \bar{u} = U_w f'(\eta), \quad \bar{w} = -\sqrt{\frac{av}{1-ct}} f(\eta), \quad \theta = \frac{\bar{T} - T_h}{T_f - T_h} \tag{24}$$

We obtain the following system of ordinary differential equations,

$$\begin{aligned}
 f^{iv} + f f''' - \frac{Sq}{2} (3f'' - \eta f''') - \left(M^2 + \frac{1}{Da} \right) f'' \\
 + \alpha \left(-2f'' f'' - f' f^{iv} - f f^{v} + \frac{Sq}{2} (5f^{iv} - \eta f^v) \right) - \gamma (2f'' f'' + f' f^{iv}) \\
 + \beta \left(7f'^3 + 24f' f'' f''' + 3f'^2 f^{iv} + \text{Re} \left(3f'' f''^2 + \frac{3}{2} f'^2 f^{iv} \right) \right) = 0,
 \end{aligned} \tag{25}$$

$$(1 + Rd)\theta'' + Pr\left(\theta'f - \frac{Sq}{2}\eta\theta'\right) + PrEc\left\{M^2f'^2 + \frac{6}{Re}f'^2 + f''^2 + \alpha\left(\frac{1}{Re}(-6f'^3 - 6ff'f'')\right)\right. \\ \left.-f'f''^2 - ff''f'' + \frac{Sq}{2}(3f''^2 + \eta f''f''') + \frac{Sq}{Re}(6f'^2 + 3\eta f'f'')\right\} \\ \left.-3\gamma\left(\frac{2f'^3}{Re} + \frac{f'f''^2}{2}\right) + \beta\left(\frac{18f'^4}{Re} + 6f'^2f''^2 + \frac{Re}{2}f''^4\right)\right\} = 0 \tag{26}$$

The corresponding boundary conditions are

$$f(0) = A, f(1) = \frac{Sq}{2}, f'(0) = 1, f'(1) = 0, \tag{27}$$

$$\theta'(0) = \Upsilon_1(\theta(0) - 1), \theta'(1) = -\Upsilon_2\theta(1) \tag{28}$$

where

$$\alpha = \frac{(\alpha_1)_{nf}a}{\mu_{nf}(1-ct)}, \beta = \frac{2(\beta_3)_{nf}a^2}{\mu_{nf}(1-ct)^2}, \gamma = \frac{(\alpha_2)_{nf}a}{\mu_{nf}(1-ct)}, Re = \frac{ar^2}{2\nu_{nf}(1-ct)}, \\ Pr = \frac{\mu_{nf}C_{p,nf}}{k_{nf}}, Ec = \frac{U_w^2}{C_{p,nf}(T_f - T_h)}, M^2 = \frac{\sigma_{nf}B_0^2}{\rho_{nf}a}, Sq = \frac{c}{a}, \tag{29} \\ A = \sqrt{\frac{(1-ct)}{av}}w_0, Rd = \frac{16\sigma_{nf}^*T_h^3}{3k_{1,nf}K}, \Upsilon_1 = \frac{h_1h(t)}{K}, \Upsilon_2 = \frac{h_2h(t)}{K}$$

3. Method of solutions using differential transformation method

It is evident that the nonlinearities in the governing equations of flow and heat transfer in Eqs. (25) and (26) make the development of exact analytical solutions for the equations very difficult, if not to say impossible. Considering the comparative advantages, provision of acceptable

analytical results with convenient convergence and stability coupled with relative simplicity of differential transformation method, the system of nonlinear differential equations in Eqs. (25) and (26) are solved using differential transformation method. The basic definition, procedure and properties can be found in our previous publications [52, 57].

Following our previous studies [57], the differential transformation or the recursive relations for the governing Eqs. (25) and (26) are;

Table 1. Physical and thermal properties of the base fluid.

Base fluid	ρ (kg/m ³)	c_p (J/kgK)	k (W/mK)
Pure water	997.1	4179	0.613

Table 2. Physical and thermal properties of nanoparticles.

Nanoparticles	ρ (kg/m ³)	c_p (J/kgK)	k (W/mK)
Copper (II) Oxide (CuO)	783	540	18

$$\left(\begin{aligned}
 &(k+1)(k+2)(k+3)(k+4)F_{k+4} + \sum_{l=0}^k (l+1)(l+2)(l+3)F_{l+3}F_{k-l} \\
 &-1/2Sq \left(3(k+1)(k+2)F_{k+2} - \sum_{l=0}^k (l+1)(l+2)(l+3)F_{l+3}\delta(k-1-l) \right) \\
 &-(M^2 + Da^{-1})(k+1)(k+2)F_{k+2} \\
 &+ \alpha \left(\begin{aligned}
 &-2 \sum_{l=0}^k (l+1)(l+2)(l+3)F_{l+3}(k-l+1)(k-l+2)F_{k-l+2} \\
 &- \sum_{l=0}^k (l+1)(l+2)(l+3)(l+4)F_{l+4}(k-l+1)F_{k-l+1} \\
 &- \sum_{l=0}^k (l+1)(l+2)(l+3)(l+4)(l+5)F_{l+5}F_{k-l} \\
 &+ 1/2Sq \left(\begin{aligned}
 &5(k+1)(k+2)(k+3)(k+4)F_{k+4} \\
 &- \sum_{l=0}^k (l+1)(l+2)(l+3)(l+4)(l+5)F_{l+5}\delta(k-1-l)
 \end{aligned} \right)
 \end{aligned} \right) \\
 &-y \left(\begin{aligned}
 &2 \sum_{l=0}^k (l+1)(l+2)(l+3)F_{l+3}(k-l+1)(k-l+2)F_{k-l+2} \\
 &+ \sum_{l=0}^k (l+1)(l+2)(l+3)(l+4)F_{l+4}(k-l+1)F_{k-l+1}
 \end{aligned} \right) \\
 &+ 7\beta \sum_{p=0}^k \left(\begin{aligned}
 &\sum_{l=0}^p (l+1)(l+2)F_{l+2}(p-l+1)(p-l+2) \\
 &F_{p-l+2}(k-p+1)(k-p+2)F_{k-p+2}
 \end{aligned} \right) \\
 &+ 24 \sum_{p=0}^k \left(\begin{aligned}
 &\sum_{l=0}^p (l+1)(l+2)(l+3)F_{l+3} \\
 &(p-l+1)(p-l+2)F_{p-l+2}(k-p+1)F_{k-p+1}
 \end{aligned} \right) \\
 &+ 3 \sum_{p=0}^k \left(\begin{aligned}
 &\sum_{l=0}^p (l+1)(l+2)(l+3)(l+4)F_{l+4} \\
 &(p-l+1)F_{p-l+1}(k-p+1)F_{k-p+1}
 \end{aligned} \right) \\
 &+ R_e \left(\begin{aligned}
 &3 \sum_{p=0}^k \left(\begin{aligned}
 &\sum_{l=0}^p (l+1)(l+2)(l+3)F_{l+3}(p-l+1) \\
 &F_{p-l+3}(k-p+1)(k-p+2)F_{k-p+2}
 \end{aligned} \right) \\
 &+ 3/2 \sum_{p=0}^k \left(\begin{aligned}
 &\sum_{l=0}^p (l+1)(l+2)(l+3)(l+4)F_{l+4} \\
 &(p-l+1)(p-l+2)F_{p-l+2}(k-p+1)(k-p+2)F_{k-p+2}
 \end{aligned} \right)
 \end{aligned} \right)
 \end{aligned} \right) = 0 \tag{30}$$

$$\begin{aligned}
 & (1 + Rd)(k + 1)(k + 2)\theta_{k+2} + \Pr \left(\sum_{l=0}^k (l + 1)\theta_{l+1}F_{k-l} - 1/2Sq \sum_{l=0}^k (l + 1)\theta_{l+1}\delta(k - 1 - l) \right) \\
 & \left(\begin{aligned}
 & M^2 \sum_{l=0}^k (l + 1)F_{l+1}(k - l + 1)F_{k-l+1} + 6 \frac{\sum_{l=0}^k (l + 1)F_{l+1}(k - l + 1)F_{k-l+1}}{R_e} \\
 & + \sum_{l=0}^k (l + 1)(l + 2)F_{l+2}(k - l + 1)(k - l + 2)F_{k-l+2} + \\
 & \left(\begin{aligned}
 & -6 \sum_{p=0}^k \left(\sum_{l=0}^p (l + 1)F_{l+1}(p - l + 1)F_{p-l+1}(k - p + 1)F_{k-p+1} \right) \\
 & -6 \sum_{p=0}^k \left(\sum_{l=0}^p (l + 1)(l + 2)F_{l+2}(p - l + 1)F_{p-l+1}F_{k-p} \right) \\
 & \frac{\hspace{10em}}{R_e} \\
 & - \sum_{p=0}^k \left(\sum_{l=0}^p (l + 1)(l + 2)F_{l+2}(p - l + 1)(p - l + 2)F_{p-l+2}(k - p + 1)F_{k-p+1} \right) \\
 & \alpha - \sum_{p=0}^k \left(\sum_{l=0}^p (l + 1)(l + 2)(l + 3)F_{l+3}(p - l + 1)(p - l + 2)F_{p-l+2}F_{k-p} \right) \\
 & + 1/2Sq \left(\begin{aligned}
 & 3 \sum_{l=0}^k (l + 1)(l + 2)F_{l+2}(k - l + 1)(k - l + 2)F_{k-l+2} \\
 & + \sum_{p=0}^k \left(\sum_{l=0}^p (l + 1)(l + 2)(l + 3)F_{l+3}(p - l + 1)(p - l + 2)F_{p-l+2}\delta(k - 1 - p) \right) \end{aligned} \right) \\
 & + \Pr Ec \left(\begin{aligned}
 & Sq \left(6 \sum_{l=0}^k (l + 1)F_{l+1}(k - l + 1)F_{k-l+1} + 3 \sum_{p=0}^k \left(\sum_{l=0}^p (l + 1)(l + 2)F_{l+2}(p - l + 1)F_{p-l+1}\delta(k - 1 - p) \right) \right) \\
 & \frac{\hspace{10em}}{R_e} \end{aligned} \right) \\
 & - 3y \left(\begin{aligned}
 & 2 \frac{\sum_{p=0}^k \left(\sum_{l=0}^p (l + 1)F_{l+1}(p - l + 1)F_{p-l+1}(k - p + 1)F_{k-p+1} \right)}{R_e} \\
 & + 1/2 \sum_{p=0}^k \left(\sum_{l=0}^p (l + 1)(l + 2)F_{l+2}(p - l + 1)(p - l + 2)F_{p-l+2}(k - p + 1)F_{k-p+1} \right) \end{aligned} \right) + \\
 & \left(\begin{aligned}
 & 18 \frac{\sum_{p=0}^k \left(\sum_{n=0}^p \left(\sum_{l=0}^n (l + 1)F_{l+1}(n - l + 1)F_{n-l+1}(p - n + 1)F_{p-n+1}(k - p + 1)F_{k-p+1} \right) \right)}{R_e} \\
 & \beta + 6 \sum_{p=0}^k \left(\sum_{n=0}^p \left(\sum_{l=0}^n (l + 1)(l + 2)F_{l+2}(n - l + 1)(n - l + 2)F_{n-l+2}(p - n + 1)F_{p-n+1}(k - p + 1)F_{k-p+1} \right) \right) \\
 & + 1/2R_e \sum_{p=0}^k \left(\sum_{n=0}^p \left(\sum_{l=0}^n (l + 1)(l + 2)F_{l+2}(n - l + 1)(n - l + 2)F_{n-l+2} \right) \right) \\
 & \left(\sum_{n=0}^p (p - n + 1)(p - n + 2)F_{p-n+2}(k - p + 1)(k - p + 2)F_{k-p+2} \right) \end{aligned} \right) \end{aligned} \right) = 0 \tag{31}
 \end{aligned}$$

where, $\delta(k) = \begin{cases} 1k = 0 \\ 0k \neq 0 \end{cases}$

After that, the other boundary conditions are represented at first. These unknowns follow the series solution and are obtained using the actual boundary condition associated with the governing equation and re-substituted back into the series solution.

Transforming and representing the boundary conditions,

$$f' = p, \tag{36}$$

$$F_0 = A, F_1 = 1, F_2 = C, F_3 = E, \dots, \theta[0] = G, \theta[1] = H, \tag{32} \quad f'' = p' = q, \tag{37}$$

$$F_4 = \frac{1}{12Da(12C^2R_e\beta + 5Sq\alpha - 2\alpha + 6\beta - 2y + 2)} \begin{pmatrix} 36CDaE^2R_e\beta + 56C^3Da\beta - 120ADa\alpha F_5 \\ -24CDaE\alpha + 288CDaE\beta - 24CDaEy \\ -2CDaM^2 + 6ADaE - 3CDaSq - 2C \end{pmatrix} \tag{33}$$

$$\theta_2 = \frac{Pr}{2R_e(1 + Ra)} \begin{pmatrix} -8C^4EcR_e^2\beta + 12ACEEcR_e\alpha - 6C^2EcR_eSq\alpha \\ +4C^2EcR_e\alpha - 24C^2EcR_e\beta + 6C^2EcR_e\gamma \\ +12ACEc\alpha - 4C^2EcR_e - EcM^2R_e - AHR_e \\ -6EcSq\alpha + 6Ec\alpha - 18Ec\beta + 6Ec\gamma - 6Ec \end{pmatrix} \tag{34}$$

$$f''' = q' = w, \tag{38}$$

$$f^{iv} = w' = z, \tag{39}$$

$$F_5 = \frac{1}{60Da} \begin{pmatrix} 1296C^2DaE^3R_e^2\beta^2 - 3456C^4DaER_e\beta^2 + 4320AC^2DaR_e\alpha\beta F_6 \\ -1080C^2DaE^2R_e\alpha\beta + 12528C^2DaE^2R_e\beta^2 - 1080C^2DaE^2R_e\beta \\ y - 72C^2DaEM^2R_e\beta - 270DaE^3R_eSq\alpha\beta + 360ACDaE^2R_e\beta \\ -336C^4Da\alpha\beta + 3360C^4Da\beta^2 - 336C^4Da\beta\gamma - 126C^2DaER_eSq\beta \\ -2700C^2DaESq\alpha\beta + 108DaE^3R_e\alpha\beta - 324DaE^3R_e\beta^2 + 108DaE^3R_e\beta\gamma \\ +56AC^3Da\beta + 1800ADaSq\alpha^2 F_6 - 36C^2DaER_e\beta + 144C^2DaE\alpha^2 \\ -2088C^2DaE\alpha\beta + 288C^2DaE\alpha\gamma + 14040C^2DaE\beta^2 - 2088C^2Da \\ E\beta\gamma + 144C^2DaEy^2 + 12C^2DaM^2\alpha - 120C^2DaM^2\beta + 12C^2DaM^2\gamma \\ -108DaE^3R_e\beta + 180DaE^2Sq\alpha^2 - 2160DaE^2Sq\alpha\beta + 180DaE^2Sq\alpha\gamma \\ +15DaEM^2Sq\alpha - 60ACDaE\alpha + 648ACDaE\beta - 60ACDaEy \\ -2ACDaM^2 - 720ADa\alpha^2 F_6 + 2160ADa\alpha\beta F_6 - 720ADa\alpha\gamma F_6 \\ +18C^2DaSq\alpha - 180C^2DaSq\beta + 18C^2DaSq\gamma - 72C^2ER_e\beta \\ -72DaE^2\alpha^2 + 1080DaE^2\alpha\beta - 144DaE^2\alpha\gamma - 2592DaE^2\beta^2 \\ +1080DaE^2\beta\gamma - 72DaE^2\gamma^2 - 6DaEM^2\alpha + 18DaEM^2\beta \\ +15DaESq^2\alpha + 6A^2DaE - 3ACDaSq + 720ADa\alpha F_6 \\ +72DaE^2\alpha - 864DaE^2\beta + 72DaE^2\gamma + 6DaEM^2 - 21DaESq\alpha \\ +18DaESq\beta - 6DaESq\gamma + 12C^2\alpha - 120C^2\beta + 12C^2\gamma + 6DaESq \\ +6DaE\alpha - 18DaE\beta + 6DaEy + 15ESq\alpha - 2AC - 6DaE \\ -6E\alpha + 18E\beta - 6E\gamma + 6E - 6DaEM^2\gamma - 1080C^2DaE\beta \end{pmatrix} \tag{35}$$

4. Numerical procedure for the analysis of the governing equation

For the purpose of verifying the solutions of DTM for the system of the governing equations in Eqs. (25) and (26), a numerical scheme based on fifth-order Runge-Kutta Fehlberg method (Cash-Karp Runge-Kutta) coupled with shooting method is developed. In order to apply the nu-

$$z = fw - \frac{Sq}{2}(3q - \eta w) - \left(M^2 + \frac{1}{Da}\right)q + \alpha \left(-2qw - pz - fz' + \frac{Sq}{2}(5z - \eta z')\right) + \gamma(2qw + pz) + \beta \left(7q^2 + 24pqw + 3p^2z + \text{Re} \left(3qw^2 + \frac{3}{2}q^2z\right)\right) = 0, \tag{40}$$

From Eq. (40), it could be established that

$$z' = \frac{\left\{ fw - \frac{Sq}{2}(3q - \eta w) - \left(M^2 + \frac{1}{Da}\right)q + \alpha \left(-2qw - pz + \frac{5Sq}{2}\right) - \gamma(2qw + pz) + \beta \left(7q^2 + 24pqw + 3p^2z + \text{Re} \left(3qw^2 + \frac{3}{2}q^2z\right)\right) - z \right\}}{\alpha \left(f + \frac{Sq}{2}\right)} \tag{41}$$

merical scheme, the fourth-order and second-order ordinary differential equations in Eqs. (25) and (26), respectively, are decomposed into a system of first-order differential equations as follows:

$$\text{The above Eqs. (36), (37), (38), (39), (40), and (41) can be written as} \\ a(\eta, f, p, q, w, z) = p, \tag{42}$$

$$b(\eta, f, p, q, w, z) = q, \tag{43}$$

$$c(\eta, f, p, q, w, z) = w, \tag{44}$$

$$d(\eta, f, p, q, w, z) = z \tag{45}$$

$$e(\eta, f, p, q, z) = \frac{\left\{ fw - \frac{Sq}{2}(3q - \eta w) - \left(M^2 + \frac{1}{Dv}\right)q + \alpha \left(-2qw - pz + \frac{5Sq}{2}\right) - \gamma(2qw + pz) + \beta \left(7q^2 + 24pqw + 3p^2z + \text{Re}\left(3qw^2 + \frac{3}{2}q^2z\right)\right) - z \right\}}{\alpha \left(f + \frac{Sq}{2}\right)} \tag{46}$$

The iterative scheme of the fifth-order Runge-Kutta Fehlberg method (Cash-Karp Runge-Kutta) for the above system of first-order equations is given as

$$f_{i+1} = f_i + h \left(\frac{2835}{27648}k_1 + \frac{18575}{48384}k_3 + \frac{13525}{55296}k_4 + \frac{277}{14336}k_5 + \frac{1}{4}k_6 \right) \tag{47}$$

$$p_{i+1} = p_i + h \left(\frac{2835}{27648}l_1 + \frac{18575}{48384}l_3 + \frac{13525}{55296}l_4 + \frac{277}{14336}l_5 + \frac{1}{4}l_6 \right) \tag{48}$$

$$q_{i+1} = q_i + h \left(\frac{2835}{27648}m_1 + \frac{18575}{48384}m_3 + \frac{13525}{55296}m_4 + \frac{277}{14336}m_5 + \frac{1}{4}m_6 \right) \tag{49}$$

$$w_{i+1} = w_i + h \left(\frac{2835}{27648}n_1 + \frac{18575}{48384}n_3 + \frac{13525}{55296}n_4 + \frac{277}{14336}n_5 + \frac{1}{4}n_6 \right) \tag{50}$$

$$z_{i+1} = z_i + h \left(\frac{2835}{27648}r_1 + \frac{18575}{48384}r_3 + \frac{13525}{55296}r_4 + \frac{277}{14336}r_5 + \frac{1}{4}r_6 \right) \tag{51}$$

where

$$k_1 = a(\eta_i, f_i, p_i, q_i, w_i, z_i)$$

$$l_1 = b(\eta_i, f_i, p_i, q_i, w_i, z_i)$$

$$m_1 = c(\eta_i, f_i, p_i, q_i, w_i, z_i)$$

$$n_1 = d(\eta_i, f_i, p_i, q_i, w_i, z_i)$$

$$r_1 = e(\eta_i, f_i, p_i, q_i, w_i, z_i)$$

$$k_2 = a \left(\eta_i + \frac{1}{5}h, f_i + \frac{1}{5}k_1h, p_i + \frac{1}{5}l_1h, q_i + \frac{1}{5}m_1h, w_i + \frac{1}{5}n_1h, z_i + \frac{1}{5}r_1h \right)$$

$$l_2 = b \left(\eta_i + \frac{1}{5}h, f_i + \frac{1}{5}k_1h, p_i + \frac{1}{5}l_1h, q_i + \frac{1}{5}m_1h, w_i + \frac{1}{5}n_1h, z_i + \frac{1}{5}r_1h \right)$$

$$m_2 = c \left(\eta_i + \frac{1}{5}h, f_i + \frac{1}{5}k_1h, p_i + \frac{1}{5}l_1h, q_i + \frac{1}{5}m_1h, w_i + \frac{1}{5}n_1h, z_i + \frac{1}{5}r_1h \right)$$

$$n_2 = d \left(\eta_i + \frac{1}{5}h, f_i + \frac{1}{5}k_1h, p_i + \frac{1}{5}l_1h, q_i + \frac{1}{5}m_1h, w_i + \frac{1}{5}n_1h, z_i + \frac{1}{5}r_1h \right)$$

$$r_2 = e \left(\eta_i + \frac{1}{5}h, f_i + \frac{1}{5}k_1h, p_i + \frac{1}{5}l_1h, q_i + \frac{1}{5}m_1h, w_i + \frac{1}{5}n_1h, z_i + \frac{1}{5}r_1h \right)$$

$$k_3 = a \left(\eta_i + \frac{3}{10}h, f_i + \frac{3}{40}k_1h + \frac{9}{40}k_2h, p_i + \frac{3}{40}l_1h + \frac{9}{40}l_2h, q_i + \frac{3}{40}m_1h + \frac{9}{40}m_2h, w_i + \frac{3}{40}n_1h + \frac{9}{40}n_2h, z_i + \frac{3}{40}r_1h + \frac{9}{40}r_2h \right)$$

$$l_3 = b \left(\eta_i + \frac{3}{10}h, f_i + \frac{3}{40}k_1h + \frac{9}{40}k_2h, p_i + \frac{3}{40}l_1h + \frac{9}{40}l_2h, q_i + \frac{3}{40}m_1h + \frac{9}{40}m_2h, w_i + \frac{3}{40}n_1h + \frac{9}{40}n_2h, z_i + \frac{3}{40}r_1h + \frac{9}{40}r_2h \right)$$

$$m_3 = c \left(\eta_i + \frac{3}{10}h, f_i + \frac{3}{40}k_1h + \frac{9}{40}k_2h, p_i + \frac{3}{40}l_1h + \frac{9}{40}l_2h, q_i + \frac{3}{40}m_1h + \frac{9}{40}m_2h, w_i + \frac{3}{40}n_1h + \frac{9}{40}n_2h, z_i + \frac{3}{40}r_1h + \frac{9}{40}r_2h \right)$$

$$n_3 = d \left(\eta_i + \frac{3}{10}h, f_i + \frac{3}{40}k_1h + \frac{9}{40}k_2h, p_i + \frac{3}{40}l_1h + \frac{9}{40}l_2h, q_i + \frac{3}{40}m_1h + \frac{9}{40}m_2h, w_i + \frac{3}{40}n_1h + \frac{9}{40}n_2h, z_i + \frac{3}{40}r_1h + \frac{9}{40}r_2h \right)$$

$$r_3 = e \left(\eta_i + \frac{3}{10}h, f_i + \frac{3}{40}k_1h + \frac{9}{40}k_2h, p_i + \frac{3}{40}l_1h + \frac{9}{40}l_2h, q_i + \frac{3}{40}m_1h + \frac{9}{40}m_2h, w_i + \frac{3}{40}n_1h + \frac{9}{40}n_2h, z_i + \frac{3}{40}r_1h + \frac{9}{40}r_2h \right)$$

$$k_4 = a \left(\eta_i + \frac{3}{5}h, f_i + \frac{3}{10}k_1h - \frac{9}{10}k_2h + \frac{6}{5}k_3h, p_i + \frac{3}{10}l_1h - \frac{9}{10}l_2h + \frac{6}{5}l_3h, q_i + \frac{3}{10}m_1h - \frac{9}{10}m_2h + \frac{6}{5}m_3h, w_i + \frac{3}{10}n_1h - \frac{9}{10}n_2h + \frac{6}{5}n_3h, z_i + \frac{3}{10}r_1h - \frac{9}{10}r_2h + \frac{6}{5}r_3h \right)$$

$$l_4 = b \left(\eta_i + \frac{3}{5}h, f_i + \frac{3}{10}k_1h - \frac{9}{10}k_2h + \frac{6}{5}k_3h, p_i + \frac{3}{10}l_1h - \frac{9}{10}l_2h + \frac{6}{5}l_3h, q_i + \frac{3}{10}m_1h - \frac{9}{10}m_2h + \frac{6}{5}m_3h, w_i + \frac{3}{10}n_1h - \frac{9}{10}n_2h + \frac{6}{5}n_3h, z_i + \frac{3}{10}r_1h - \frac{9}{10}r_2h + \frac{6}{5}r_3h \right)$$

$$m_4 = c \left(\eta_i + \frac{3}{5}h, f_i + \frac{3}{10}k_1h - \frac{9}{10}k_2h + \frac{6}{5}k_3h, p_i + \frac{3}{10}l_1h - \frac{9}{10}l_2h + \frac{6}{5}l_3h, q_i + \frac{3}{10}m_1h - \frac{9}{10}m_2h + \frac{6}{5}m_3h, w_i + \frac{3}{10}n_1h - \frac{9}{10}n_2h + \frac{6}{5}n_3h, z_i + \frac{3}{10}r_1h - \frac{9}{10}r_2h + \frac{6}{5}r_3h \right)$$

Table 3. Numerical values of skin friction for different parameter

A	γ	β	Re	M	S_q	A	RKFM	HAM	DTM
							[81]		
							$\frac{1}{-Re^2 C_f}$	$\frac{1}{-Re^2 C_f}$	$\frac{1}{-Re^2 C_f}$
0.01	0.10	0.10	1.00	0.40	1.00	0.01	3.88243	3.88243	3.88243
0.02							3.95950	3.95950	3.95950
0.03							4.03655	4.03655	4.03655
0.01	0.11						3.85249	3.85249	3.85249
	0.12						3.82255	3.82255	3.82255
	0.13						3.79260	3.79260	3.79260
	0.10	0.20					4.63884	4.63884	4.63884
		0.25					5.02298	5.02298	5.02298
		0.29					5.33196	5.33196	5.33196
		0.10	0.10				3.85868	3.85868	3.85868
			0.20				3.86116	3.86116	3.86116
			0.30				3.86368	3.86368	3.86368
			1.00	0.50			3.90088	3.90088	3.90088
				0.60			3.92337	3.92337	3.92337
				0.70			3.94985	3.94985	3.94985
				0.40	0.70		6.41631	6.41631	6.41631
					0.75		6.00413	6.00413	6.00413
					0.80		5.58953	5.58953	5.58953
					1.00	0.02	4.06568	4.06568	4.06568
						0.03	4.24817	4.24817	4.24817
						0.04	4.42993	4.42993	4.42993

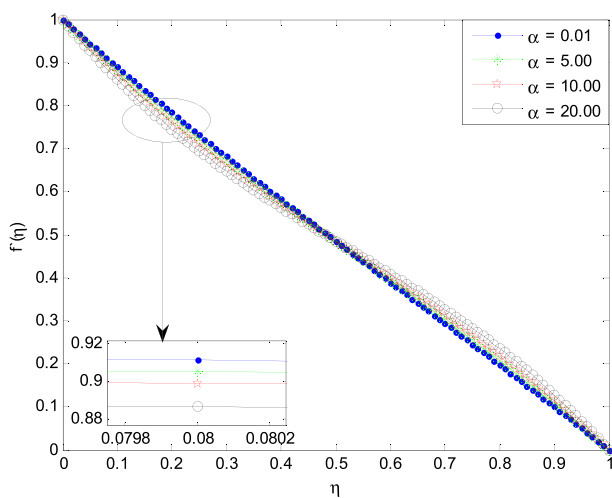


Figure 2. Effect of α on dimensionless velocity profile.

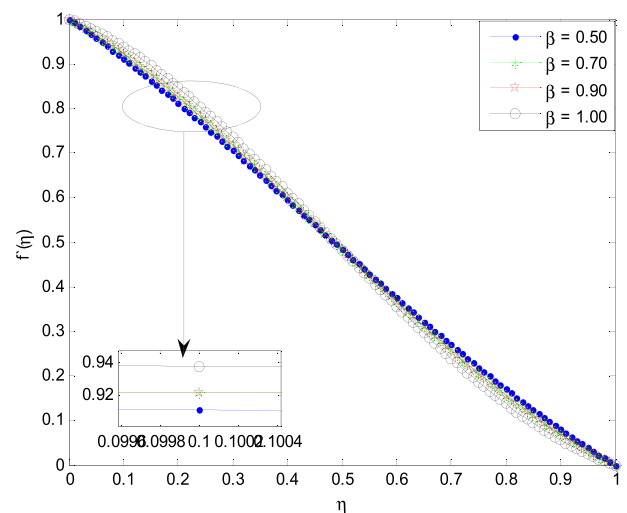


Figure 3. Effect of β on dimensionless velocity profile.

$$n_4 = d \begin{pmatrix} \eta_i + \frac{3}{5}h, f_i + \frac{3}{10}k_1h - \frac{9}{10}k_2h + \frac{6}{5}k_3h, p_i + \frac{3}{10}l_1h - \frac{9}{10}l_2h + \frac{6}{5}l_3h, \\ q_i + \frac{3}{10}m_1h - \frac{9}{10}m_2h + \frac{6}{5}m_3h, w_i + \frac{3}{10}n_1h - \frac{9}{10}n_2h + \frac{6}{5}n_3h, \\ z_i + \frac{3}{10}r_1h - \frac{9}{10}r_2h + \frac{6}{5}r_3h \end{pmatrix}$$

$$r_4 = e \begin{pmatrix} \eta_i + \frac{3}{5}h, f_i + \frac{3}{10}k_1h - \frac{9}{10}k_2h + \frac{6}{5}k_3h, p_i + \frac{3}{10}l_1h - \frac{9}{10}l_2h + \frac{6}{5}l_3h, \\ q_i + \frac{3}{10}m_1h - \frac{9}{10}m_2h + \frac{6}{5}m_3h, w_i + \frac{3}{10}n_1h - \frac{9}{10}n_2h + \frac{6}{5}n_3h, \\ z_i + \frac{3}{10}r_1h - \frac{9}{10}r_2h + \frac{6}{5}r_3h \end{pmatrix}$$

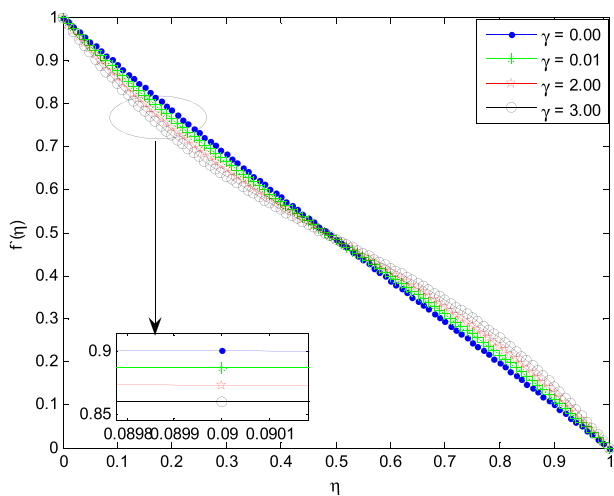


Figure 4. Effect of γ on dimensionless velocity profile.

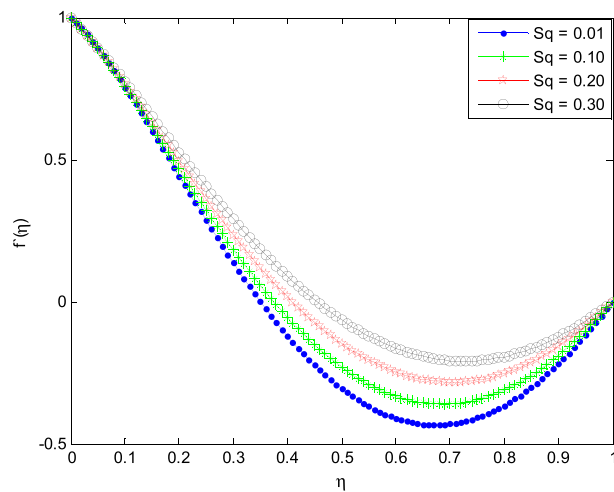


Figure 7. Effect of squeezing term on dimensionless velocity profile.

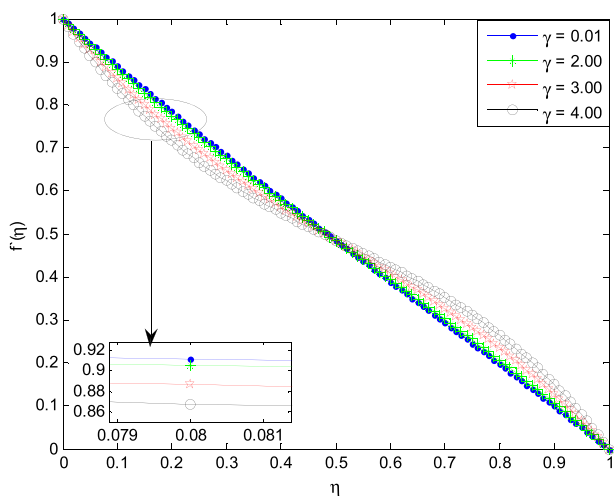


Figure 5. Effect of γ on dimensionless velocity profile.

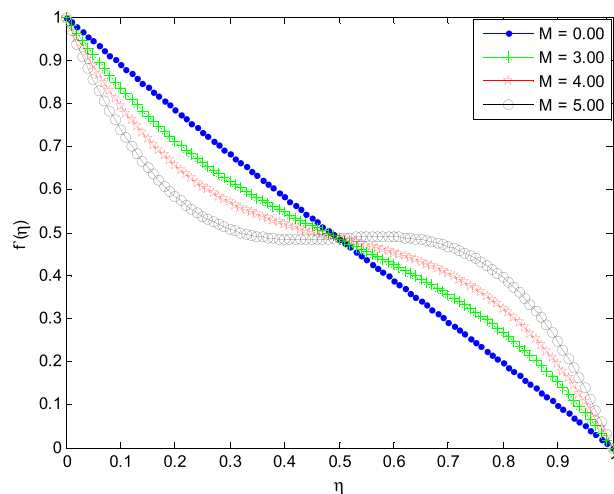


Figure 8. Effect of Hartman number on dimensionless velocity profile.

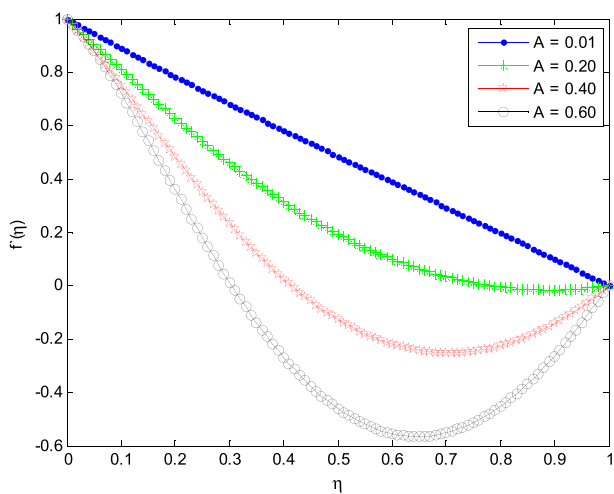


Figure 6. Effect of suction term on dimensionless velocity profile.

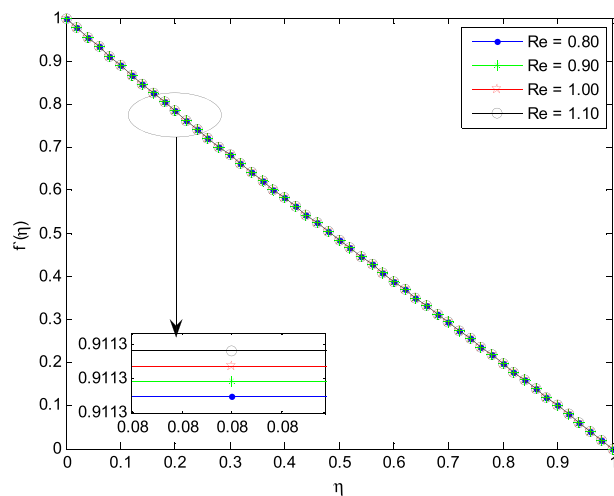


Figure 9. Effect of Reynold's number on dimensionless velocity profile.

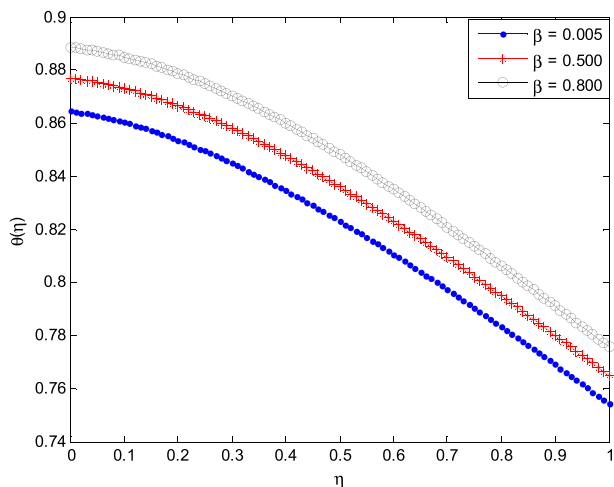


Figure 10. Effect of the third grade fluid parameter on Dimensionless temperature profile.

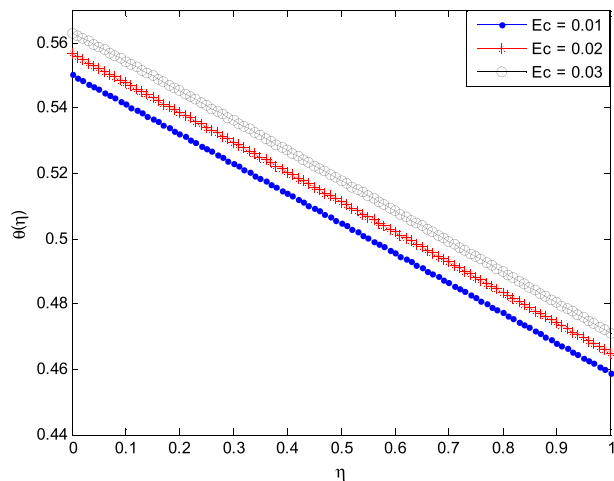


Figure 13. Effect of Eckert number on dimensionless temperature profile.

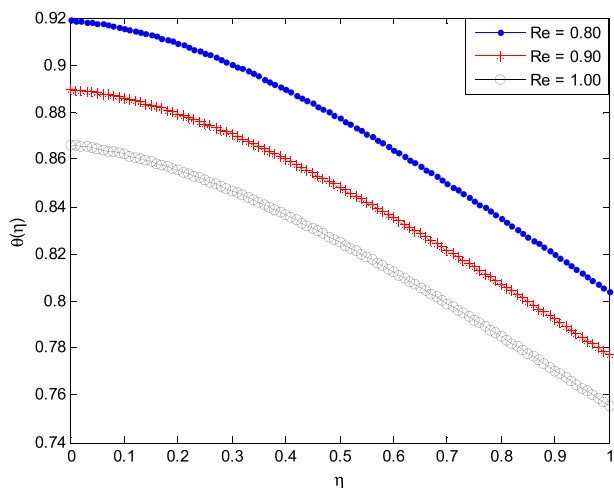


Figure 11. Effect of Reynold's number on dimensionless Dimensionless temperature profile.

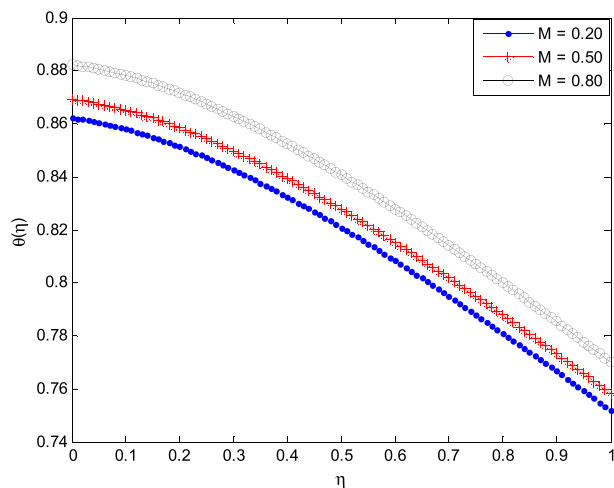


Figure 14. Effect of Hartman number on dimensionless temperature profile.

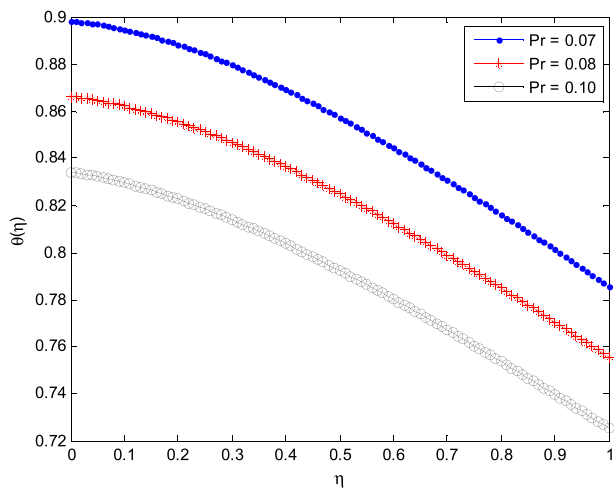


Figure 12. Effect of Prandtl number on dimensionless temperature profile.

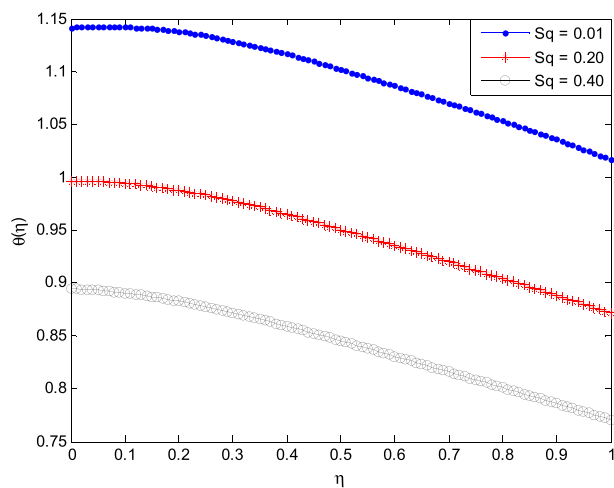


Figure 15. Effect of squeezing parameter on dimensionless temperature profile.

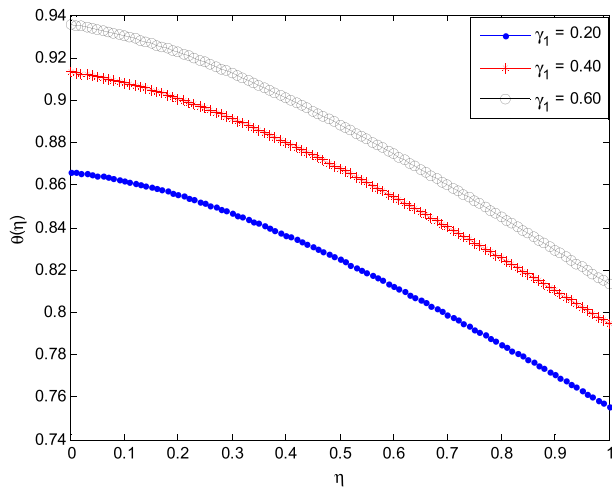


Figure 16. Effect of the first thermal Biot number on dimensionless temperature profile.

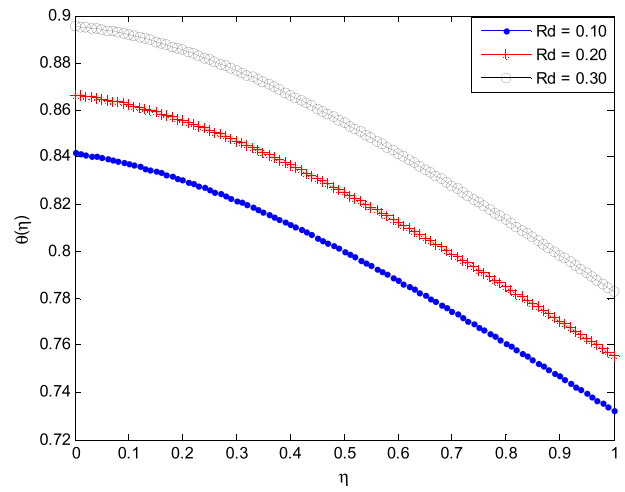


Figure 18. Effect of Radiation term on dimensionless temperature profile.

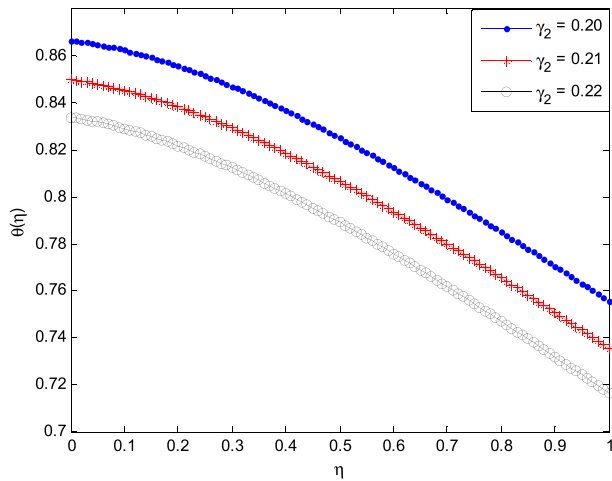


Figure 17. Effect of the second thermal Biot number on dimensionless temperature profile.

$$k_5 = a \begin{pmatrix} \eta_i + h, f_i - \frac{11}{54}k_1h + \frac{5}{2}k_2h - \frac{70}{27}k_3h + \frac{35}{27}k_4h, p_i - \frac{11}{54}l_1h + \frac{5}{2}l_2h - \frac{70}{27}l_3h + \frac{35}{27}l_4h, \\ q_i - \frac{11}{54}m_1h + \frac{5}{2}m_2h - \frac{70}{27}m_3h + \frac{35}{27}m_4h, w_i - \frac{11}{54}n_1h + \frac{5}{2}n_2h - \frac{70}{27}n_3h + \frac{35}{27}n_4h, \\ z_i - \frac{11}{54}r_1h + \frac{5}{2}r_2h - \frac{70}{27}r_3h + \frac{35}{27}r_4h \end{pmatrix}$$

$$l_5 = b \begin{pmatrix} \eta_i + h, f_i - \frac{11}{54}k_1h + \frac{5}{2}k_2h - \frac{70}{27}k_3h + \frac{35}{27}k_4h, p_i - \frac{11}{54}l_1h + \frac{5}{2}l_2h - \frac{70}{27}l_3h + \frac{35}{27}l_4h, \\ q_i - \frac{11}{54}m_1h + \frac{5}{2}m_2h - \frac{70}{27}m_3h + \frac{35}{27}m_4h, w_i - \frac{11}{54}n_1h + \frac{5}{2}n_2h - \frac{70}{27}n_3h + \frac{35}{27}n_4h, \\ z_i - \frac{11}{54}r_1h + \frac{5}{2}r_2h - \frac{70}{27}r_3h + \frac{35}{27}r_4h \end{pmatrix}$$

Table 4. Numerical values of Nusselt number for different parameter

α	γ	β	Sq	Pr	Ec	γ_1	γ_2	Rd	RKFM	HAM	DTM
									Nu	Nu [81]	Nu
0.01	0.10	0.10	1.00	0.10	0.10	0.20	0.20	0.20	0.092034	0.092034	0.092034
0.02									0.091945	0.091945	0.091945
0.03									0.091856	0.091856	0.091856
0.01	0.11								0.092149	0.092149	0.092149
	0.12								0.092265	0.092265	0.092265
	0.13								0.092380	0.092380	0.092380
	0.10	0.20							0.088806	0.088806	0.088806
		0.25							0.087186	0.087186	0.087186
		0.29							0.085563	0.085563	0.085563
		0.10	0.70						0.093319	0.093319	0.093319
			0.75						0.092502	0.092502	0.092502
			0.80						0.093528	0.093528	0.093528
			1.00	0.11					0.090331	0.090331	0.090331
				0.12					0.088628	0.088628	0.088628
				0.13					0.086926	0.086926	0.086926
				0.10	0.15				0.083306	0.083306	0.083306
					0.25				0.065851	0.065851	0.065851
					0.35				0.048396	0.048396	0.048396
					0.10	0.30			0.108540	0.108540	0.108540
						0.40			0.119230	0.119230	0.119230
						0.50			0.126720	0.126720	0.126720
						0.20	0.70		0.090240	0.090240	0.090240
							0.80		0.092731	0.092731	0.092731
							0.90		0.094174	0.094174	0.094174
							0.20	0.30	0.101120	0.101120	0.101120
								0.40	0.110210	0.110210	0.110210
								0.50	0.119300	0.119300	0.119300

$$r_6 = e \begin{pmatrix} \eta_i + \frac{7}{8}h, f_i + \frac{1631}{55296}k_1h + \frac{175}{512}k_2h + \frac{575}{13824}k_3h + \frac{44275}{110592}k_4h + \frac{253}{4096}k_5h, \\ p_i + \frac{1631}{55296}l_1h + \frac{175}{512}l_2h + \frac{575}{13824}l_3h + \frac{44275}{110592}l_4h + \frac{253}{4096}l_5h, \\ q_i + \frac{1631}{55296}m_1h + \frac{175}{512}m_2h + \frac{575}{13824}m_3h + \frac{44275}{110592}m_4h + \frac{253}{4096}m_5h, \\ n_i + \frac{1631}{55296}w_1h + \frac{175}{512}w_2h + \frac{575}{13824}w_3h + \frac{44275}{110592}w_4h + \frac{253}{4096}w_5h, \\ z_i + \frac{1631}{55296}r_1h + \frac{175}{512}r_2h + \frac{575}{13824}r_3h + \frac{44275}{110592}r_4h + \frac{253}{4096}r_5h \end{pmatrix}.$$

Using the above fifth-order Runge-Kutta Fehlberg method coupled with shooting method, computer programs are written in MATLAB for the numerical solutions of Eqs. (25) and (26). The numerical results for a step size, $h = 0.01$ are compared with the results of the DTM as presented in Table 3.

5. Fluid flow and heat transfer parameters of engineering interests

In the fluid flow and heat transfer analysis, there are some important parameters which are of great interests in the engineering analysis of the thermal-fluidic studies. These set of important considerations include skin friction coefficient and Nusselt number.

5.1. Skin friction

The local skin friction coefficient at lower disk is

$$C_f = \frac{\tau_w|_{z=0}}{\frac{1}{2}\rho U_w^2} \tag{52}$$

Using the similarity variables in Eq. (24) and the dimensionless parameters in Eq. (29), one obtains the local skin friction coefficient as

$$C_f = \sqrt{2}\text{Re}^{-0.5} \left(2f''(0) + \alpha(3Sqf''(0) - 2Af'''(0) + 2f''(0)) - 2\gamma f''(0) + \beta \left(\frac{\text{Re}}{4} f'''(0) + 6f''(0) \right) \right) \tag{53}$$

5.2. Nusselt number

The local Nusselt number at the disk is

$$Nu = \frac{h(t)q_w}{K(T_f - T_h)}|_{z=0}. \tag{54}$$

where wall heat flux is defined as:

$$q_w|_{z=0} = -K \frac{\partial T}{\partial z}|_{z=0} + q_r|_{z=0}. \tag{55}$$

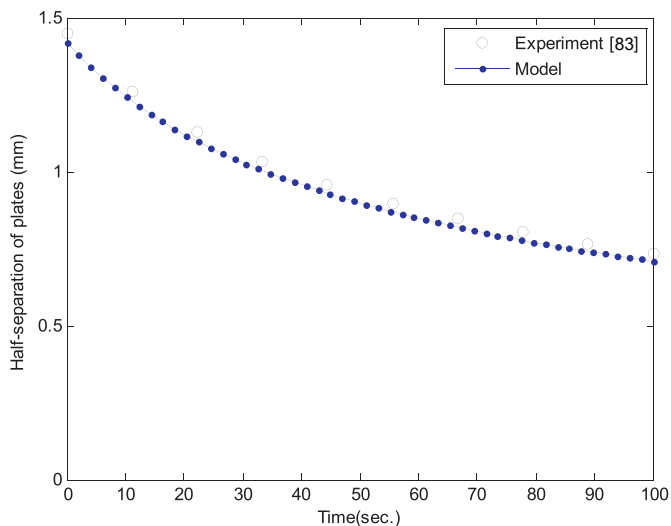


Figure 19. Comparison of experimental and the present model results.

Also, with the help of the similarity variables in Eq. (24) and the dimensionless parameters in Eq. (29), we arrived at the Nusselt number as

$$Nu = (1 + Rd)\theta'(0) \quad (56)$$

6. Results and discussion

The results of differential transformation method (DTM) and the developed fifth-order Runge-Kutta Fehlberg method (RKFM) coupled with shooting method are presented in Table 3. Parametric studies are carried out and the influences of various parameters on the flow and heat transfer processes are established as shown in Figures 2, 3, 4, 5, 6, 7, 8, 9, 10, 11, 12, 13, 14, 15, 16, 17, and 18 (see Table 4).

6.1. Effect of the third grade fluid parameters on dimensionless velocity profile

The impacts of the flow parameters on the dimensionless velocity profile of the fluid are shown in Figures 1, 2, 3, and 4. It is evident that an increase in the fluid flow parameters of the squeezing flow causes a corresponding increase in the fluid flow velocity. This is because the fluid flow parameters in question vary inversely with the viscosity of the fluid being squeezed. As these parameters increase, the viscosity of the fluid decreases and consequently increases the velocity of the fluid as the molecules of the squeezing flow are free to move with less restriction. These parameters can be used as a monitoring agent as they directly affect the viscosity of the third grade squeezing fluid.

6.2. Impacts of suction and squeezing parameters on dimensionless velocity profile

Figures 6 and 7 present the impacts of suction and squeezing parameters on dimensionless velocity profile. Figure 6 shows how the suction parameter affects the velocity of the squeezing discs for an increasing value of the fluid parameters. It is obvious that for a suction parameter greater than zero, the radial velocity of the lower disc increases while that of the upper disc decreases as a result of a corresponding increase in the viscosity of the third grade fluid from the lower squeezing disc to the upper disc. Figure 7 depicts the impact of the squeezing parameter on the fluid flow between the parallel discs. The figure shows that an increase in the squeezing parameter causes a corresponding increase in the squeezing rate. This is because as the squeezing parameter increases, the radial velocity of the squeezing discs

increases there by generating a driving compressive rotary force on the fluid flowing between the two parallel discs.

6.3. Impacts of Hartman and Reynold's numbers on dimensionless velocity profile

Figures 8 and 9 illustrates the influence of Hartman number and Reynold's numbers on dimensionless velocity profile. Figure 8 shows how the Hartman number affects the velocity of the squeezing discs for an increasing value of the fluid parameters. It is obvious that for a Hartman number greater than zero or for an increasing Hartman number, the radial velocity of the lower disc decreases while that of the upper disc increases as a result of a corresponding increase in the viscosity of the third grade fluid from the upper disc to the lower squeezing disc. As the Hartman number becomes large, it automatically raises the magnetic field as a result of a corresponding increase in the Lorentz force, hence decreases the flow velocity while increase in Reynold's number increases the velocity of the fluid as shown in Figure 9.

6.4. Impacts of the third grade fluid parameter and Reynold's number on dimensionless temperature profile

Figures 10 and 11 depict the influence of the third grade fluid parameter and Reynold's number on dimensionless temperature profile. It has been ascertained that an increase in the third grade fluid parameter causes reduction in the fluid viscosity thereby increasing resistance between the fluid molecules. However, as the Reynold's number associated with the third grade fluid increases, a decreasing effect is noticed in the dimensionless temperature profile. This is because there is a reduction in the convective capability of a high velocity fluid as compare to that with a moderate velocity.

6.5. Effects of Prandtl and Eckert numbers on dimensionless temperature profile

Figures 12 and 13 show the influence of Prandtl and Eckert numbers on dimensionless temperature profile. Figure 12 depicts a decrease in temperature profile as the Prandtl number increases. This is because an increase in the Prandtl number reduces thermal diffusivity thereby reducing the temperature profile. In Figure 13, Eckert number is observed to have a linear increasing property on the dimensionless temperature profile. This is because of the increase in the total kinetic energy of the fluid which correspondingly elevate the fluid temperature.

6.6. Impacts of Hartman number and squeezing parameter on dimensionless temperature profile

Figures 14 and 15 present the influence of Hartman number and Squeezing parameter on dimensionless temperature profile. It is clear that as the Hartman number becomes large, it automatically raises the magnetic field as a result of an increase in the Lorentz force. This makes the temperature profile to increase as the Hartman number increases. Considering Figure 15, a rapid increase in the dimensionless temperature profile is noticed for a large value of squeezing parameter as a result of a driving compressive rotary force which generates a noticeable heating effect thereby increasing the temperature profile.

6.7. Effects of the thermal Biot number and radiation term on dimensionless temperature profile

Figures 16, 17, and 18 depict the influence of the thermal Biot number and Radiation term on dimensionless temperature profile. In Figures 16 and 17, the two thermal Biot number have opposing effect on the dimensionless temperature profile but the cooling effect generated by the first Biot number is more that the temperature rising effect obtained from the second even for the same range of values. As a result, these

parameters can serve as a control for temperature monitoring. However, in Figure 18, as the radiation parameter increases, the dimensionless temperature profile increases. This is because, an increase in the radiation property causes a reduction in the absorptivity and consequently increases the rate of heat transfer to the third grade fluid.

6.8. Validation of the developed models and the solutions

Although, experimental studies on flow analyses of third grade fluids are not common, there are various examples of fluid which exhibit the characteristics of third grades fluids have been given in literature. These include dilute polymer solution (polyisobutane, methylmethacrylate in n-butyl acetate), molten plastics, food rheology polymers mixed with melts, manufacturing oils and polymer melts like high viscosity silicon oils, blood, slurries etc. Zhang et al. [82] and Grimm [83] presented experimental studies on the flow analyses of polymer melts and liquids, respectively. The comparison of the present study and the experimental work of Zhang et al. [83] is shown in Figure 19 as shown. The agreement of the results of the present study and the experimental work shows the validation of the models used in this work to study the flow behaviour of the fluid.

7. Conclusion

In this study, differential transformation method has been applied to carry out nonlinear analysis of unsteady squeezing flow and heat transfer of a third grade nanofluid between two parallel disks embedded in a porous medium under the influences of thermal radiation and temperature jump boundary conditions. The developed flow and thermal models were also solved numerically using a fifth-order Runge-Kutta Fehlberg method (Cash-Karp Runge-Kutta) coupled with shooting method. Also, the influences of various flow and heat transfer parameters were investigated. The agreement of the results of the present study and the experimental work shows the validation of the models used in this work to study the flow behaviour of the fluid. Important significance of study includes the study of flow and heat transfer of third grade fluid as applied in energy conservation, coal slurries, polymer solutions, textiles, ceramics, catalytic reactors, oil recovery applications, friction reduction and micro mixing biological samples.

Declarations

Author contribution statement

M. G. Sobamowo: Conceived and designed the experiments; Analyzed and interpreted the data; Wrote the paper.

A. A. Yinusa: Contributed reagents, materials, analysis tools or data; Wrote the paper.

S.T. Aladenusi: Contributed reagents, materials, analysis tools or data.

Funding statement

This research did not receive any specific grant from funding agencies in the public, commercial, or not-for-profit sectors.

Competing interest statement

The authors declare no conflict of interest.

Additional information

No additional information is available for this paper.

Acknowledgements

We thank the members of Herzer Research Group for their moral supports towards the successful implementation and completion of this work.

References

- [1] M. Mustafa, T. Hayat, S. Obadiat, On heat and mass transfer in the unsteady squeezing flow between parallel plates, *Mechanica* 47 (2012) 1581–1589.
- [2] T. Hayat, A. Yousaf, M. Mustafa, S. Obadiat, MHD squeezing flow of second grade fluid between two parallel disk, *Int. J. Numer. Fluids* 69 (2011) 399–410.
- [3] G. Domairy, A. Aziz, Approximate analysis of MHD squeeze flow between two parallel disks with suction or injection by homotopy perturbation method", *Math. Probl Eng.* (2009).
- [4] A.M. Siddiqui, S. Irum, A.R. Ansari, Unsteady squeezing flow of a viscous MHD fluid between parallel plates, *Math. Model. Anal.* 13 (2008) 565–576.
- [5] A.M. Rashidi, H. Shahmohamadi, S. Dinarvand, Analytic approximate solutions for unsteady two dimensional and axisymmetric squeezing flows between parallel plates", *Math. Probl Eng.* (2008).
- [6] W.A. Khan, A. Aziz, Natural convective boundary layer flow over a vertical plate with uniform surface heat flux", *Int. J. Therm. Sci.* 50 (2011) 1207–1217.
- [7] W.A. Khan, A. Aziz, Double diffusive natural convection boundary layer flow in a porous medium saturated with a nanofluid over a vertical plate, prescribed surface heat, solute and nanofluid fluxes, *Int. J. Therm. Sci.* 50 (2011) 2154–2160.
- [8] A.J. Kuznetsov, N.D. Nield, Natural convective boundary layer flow of a nanofluid past a vertical plate, *Int. J. Therm. Sci.* 49 (2010) 243–247.
- [9] M.R. Hashimi, T. Hayat, A. Alsaedi, On the analytic solutions for squeezing flow of nanofluids between parallel disks, *Nonlinear Anal. Model. Contr.* 17 (4) (2014) 418–430.
- [10] M. Turkyilmazoglu, Flow and heat simultaneously induced by two stretchable rotating disks, *Phys. Fluids* 28 (2016), 043601-1-11.
- [11] V.B. Awati, O.D. Makinde, M. Jyoti, Computer extended series solution for laminar flow between a fixed impermeable disk and a porous rotating disk, *Eng. Comput.* 35 (4) (2018) 1655–1674.
- [12] P. Sibanda, O.D. Makinde, On steady MHD flow and heat transfer due to a rotating disk in a porous medium with Ohmic heating and viscous dissipation, *Int. J. Numer. Methods Heat Fluid Flow* 20 (No. 3) (2010) pp269–285.
- [13] O.D. Makinde, R.J. Moitsheki, On non-perturbative techniques for thermal radiation effect on natural convection past a vertical plate embedded in a saturated porous medium, *Math. Probl Eng.* 689074 (11pp) (2008) 2008.
- [14] A.S. Dogonchi, JChamkha Ali, S.M. Seyyedi, D.D. Ganji, Radiative nanofluid flow and heat transfer between parallel disks with penetrable and stretchable walls considering Cattaneo–Christov heat flux model, *Heat Tran. Asian Res.* 47 (2018) 735–753.
- [15] Md. JashimUddinO, AnwarBégMd, Nazir Uddin, Energy conversion under conjugate conduction, magneto-convection, diffusion and nonlinear radiation over a non-linearly stretching sheet with slip and multiple convective boundary conditions, *Energy* 115 (Part 1) (15 November 2016) 1119–1129.
- [16] T Zohra, T Fatema, M Jashim Uddin, M Ismail, A Izani, O Anwar Bég. Bioconvective electromagnetic nanofluid transport from a wedge geometry: simulation of smart electro-conductive bio-nanopolymer processing. *Heat Tran. Asian Res.* 47 (1), 231–250.
- [17] F.T. Zohra, M.J. Uddin, A.I.M. Ismail, O.A. Bég, A. Kadir, Anisotropic slip magneto-bioconvection flow from a rotating cone to a nanofluid with Stefan blowing effects, *Chin. J Phys. Taipei* 56 (1) (2017).
- [18] MJ Uddin, WA Khan, FT Zohra, AIM Ismail. Blasius and Sakiadis slip flows of nanofluid with radiation effects. *J. Aero. Eng.* 29 (4), 04015080
- [19] K.V.S. Raju, T. Sudhakar Reddy, M.C. Raju, P.V. Satya Narayana, S. Venkataramana, MHD convective flow through porous medium in a horizontal channel with insulated and impermeable bottom wall in the presence of viscous dissipation and Joule heating, *Ain Shams Eng. J.* 5 (2014) 543–551.
- [20] L.Bühler, C.Mistrangelo and T.Najuch. Magnetohydrodynamic flows in model porous structures. *Fusion Eng. Des., Volumes* 98–99.
- [21] C. GeindreauJ. L. Aurialt. Magnetohydrodynamic flow through porous media. *Ecoulement magnétohydrodynamique en milieu poreux. Comptes Rendus de l'Académie des Sciences - Series IIB - Mechanics*
- [22] J.A. Falade, Joel C. Ukaegbu, A.C. Egere, Samuel O. Adesanya, MHD oscillatory flow through a porous channel saturated with porous medium, *Alexandria Eng. J.* 56 (2017) 147–152.
- [23] J.R. Pattanaik, G.C. Dash, S. Singh, Radiation and mass transfer effects on MHD flow through porous medium past an exponentially accelerated inclined plate with variable temperature, *Ain Shams Eng. J.* 8 (2017) 67–75.
- [24] F. Ali, A. Khan, I. Khan, S. Shafie, Effects of wall shear stress on MHD conjugate flow over an inclined plate in a porous medium with ramped wall temperature, *Hindawi Publishing Corporation, Mathematical Problems in Eng.* 2014. Article ID 861708, 15 pages.
- [25] A. Khan, I. Khan, F. Ali, S. Shafie, Effects of wall shear stress on MHD conjugate flow over an inclined plate in a porous medium with ramped wall temperature. *Hindawi Publishing Corporation, Mathematical Problems in Eng.* 2014. Article ID 861708, 15 pages.
- [26] Z. Ismail, I. Khan, N.M. Nasir, R. Jusoh Awang, M.Z. Salleh, S. Shafie, The effects of magnetohydrodynamic and radiation on flow of second grade fluid past an infinite inclined plate in porous medium, in: *Proceedings of AIP conference* 1643, 2015, p. 563.

- [27] Z. Ismail, A. Khan I, A.Q. Mohamad, S. Shafie, Second grade fluid for rotating MHD of an unsteady free convection flow in a porous medium, *Defect Diffusion Forum* 362 (2015) 100–107.
- [28] Z. Ismail, I. Khan, Shafie S. Rotation and heat absorption effects on unsteady MHD free convection flow in a porous medium past an infinite inclined plate with ramped wall temperature. *Recent Adv. Math.*
- [29] M. Hatami, J. Hatami, D.D. Ganji, Computer simulation of MHD blood conveying gold nanoparticles as a third grade non-Newtonian nanofluid in a hollow porous vessel, *Comp. Method Program Biomed.* 113 (2014) 632–641.
- [30] A. Malvandi, D. D Ganji, Magnetic field effect on nanoparticles migration and heat transfer of water/alumina nanofluid in a channel, *J. Magn. Magn Mater.* 362 (2014) 172–179.
- [31] M. Sheikholeslami, M. Hatami, D.D. Ganji, Analytical Investigation of MHD Nanofluid Flow in a Semi-porous Channel, *Powder Technology*, 2013, p. 10.
- [32] M. Fakour, A. Vahabzadeh, D.D. Ganji, M. Hatami, Analytical study of micropolar fluid flow and heat transfer in a channel with permeable walls, *J. Mol. Liquids* (2015) 7.
- [33] M. Jashim, O. Uddin, A. Beg, A. I. MD, Ismail, Mathematical Modeling of Radiative Hydromagnetic Thermosolute Nanofluid Convection Slip Flow in Saturated Porous media, *Hindawi Pub. Corp.*, 2014, p. 11.
- [34] T. Hayat, M. U Qureshi, Q. Hussain, Effect of heat transfer on the peristaltic flow of an electrically conducting fluid in a porous space, *Appl. Math. Model.* 33 (4) (2009) 1862–1873.
- [35] M. Hatami, R. Nouri, D.D. Ganji, Forced convection analysis for MHD Al_2O_3 -water nanofluid flow over a horizontal plate, *J. Mol. Liquids* 187 (2013) 294–301.
- [36] M. Hatami, D.D. Ganji, Heat transfer and nanofluid flow in suction and blowing process between parallel disks in presence of variable magnetic field, *J. Mol. Liquids* 190 (2013) 159–168.
- [37] M. Sheikholeslami, M. Gorji-Bandpy, R. Ellahi, M. Hassan, S. Soleimani, Effects of MHD on Cu water nano fluid flow and heat transfer by means of CVFEM, *J. Magn.and Magnet. Mater.* 349 (2014) 188–200.
- [38] M. Sheikholeslami, M. Gorji-Bandpy, D.D. Ganji, Magnetic field effects on natural convection around a horizontal circular cylinder inside a square enclosure filled with nanofluid, *Int. Commun. Heat Mass Tran.* 39 (7) (2012) 978–986.
- [39] M. Sheikholeslami, M. Gorji-Bandpy, D.D. Ganji, S. Soleimani, Heat flux boundary condition for nanofluid filled enclosure in presence of magnetic field, *J. Mol. Liquids* 193 (2014) 174–184.
- [40] M. Sheikholeslami, M. G-Bandpy, D.D. Ganji, S. Soleimani, Effect of a magnetic field on natural convection in an enclosure between a circular and sinusoidal cylinder in the presence of magnetic field, *Int. Commun. Heat Mass Tran.* 39 (9) (2012) 1435–1443.
- [41] M. Sheikholeslami, M.G. Bandpy, Free convection of ferrofluid in a cavity heated from below in the presence of an external magnetic field, *Powder Technol.* 256 (2014) 490–498.
- [42] M. Sheikholeslami, K. Vajravelu, M.M. Rashidi, Forced convection heat transfer in a semi annulus under the influence of a variable magnetic field, *Int. J. Heat Mass Tran.* 92 (2016) 339–348.
- [43] M. Sheikholeslami, M. G-Bandpy, D.D. Ganji, P. Rana, S. Soleimani, "Magneto-hydrodynamics free convection of Al_2O_3 -water nanofluid considering thermophoresis and Brownian motion effects, *Comput. Fluid* 94 (2014) 147–160.
- [44] M. Sheikholeslami, D.D. Ganji, M.Y. Javed, R. Ellahi, Effect of thermal radiation on magneto-hydrodynamics nanofluid flow and heat transfer by means of two phase model, *J. Magn. Magn Mater.* 374 (2015) 36–43.
- [45] T. Hayat, T. Muhammad, A. Alsaedi, M.S. Alhuthali, Magneto-hydrodynamics three-dimensional flow of viscoelastic nanofluid in the presence of nonlinear thermal radiation, *J. Magn. Magn Mater.* 385 (2015) 222–229.
- [46] T. Hayat, M. Rashid, M. Imtiaz, A. Alsaedi, Magneto-hydrodynamics (MHD) flow of Cu-water nanofluid due to a rotating disk with partial slip, *AIP Adv.* 5 (2015), 067169.
- [47] T. Hayat, F.M. Abbasi, M. Al-Yami, S. Monaquel, Slip and Joule heating effects in mixed convection peristaltic transport of nanofluid with Soret and Dufour effects, *J. Mol. Liquids* 194 (2014) 93–99.
- [48] M.M. Rashidi, N. Vishnu Ganesh, A.K. Abdul Hakeem, B. Ganga, Buoyancy effect on MHD flow of nanofluid over a stretching sheet in the presence of thermal radiation, *J. Mol. Liquids* 198 (2014) 234–238.
- [49] Z. Mehrez, A. ElCafsi, A. Belghith, P. LeQuérés, MHD effects on heat transfer and entropy generation of nanofluid flow in an open cavity, *J. Magn. Magn Mater.* 374 (2015) 214–224.
- [50] F. Mabood, W.A. Khan, A.I.M. Ismail, MHD boundary layer flow and heat transfer of nanofluids over a nonlinear stretching sheet: a numerical study, *J. Magn. Magn Mater.* 374 (2015) 569–576.
- [51] F.M. Abbasi, S.A. Shehzad, T. Hayyat, A. Alsadi, M.A. Obid, Influence of heat and mass flux conditions in Hydromagnetic flow of Jeffrey nanofluid, *AIP Adv.* 5 (2015), 037111.
- [52] M.G. Sobamowo, A.A. Yinusa, M.O. Oyekeye, S.S. Folorunsho, Nonlinear analysis of a large-amplitude forced harmonic oscillation system using differential transformation method-Padé approximant technique, *World Sci. News* 140 (2020) 139–155. Published by Ministry of Science and Higher Education, Poland.
- [53] M.G. Sobamowo, L.O. Jayesimi, M.A. Waheed, Magneto-hydrodynamic squeezing flow analysis of nanofluid under the effect of slip boundary conditions using variation of parameter method, *Karbala Int. J. Modern Sci.* 4 (2018) 107–118.
- [54] M.G. Sobamowo, A.T. Akinshilo, A.A. Yinusa, Thermo- magneto-solutal squeezing flow of nanofluid between two parallel disks embedded in a porous medium: effects of nanoparticle geometry, slip, and temperature jump conditions, *Modeling Simulat. Eng.* (2018) 18. Article ID 7364634.
- [55] M.G. Sobamowo, L.O. Jayesimi, M.A. Waheed, Axisymmetric Magneto-hydrodynamic Squeezing flow of nanofluid in a porous medium under the influence of slip boundary conditions, *Transp. Phenom. Nano Micro Scales* 6 (2) (2018) 122–132.
- [56] M.G. Sobamowo, A.T. Akinshilo, Analysis of flow, heat transfer and entropy generation in a pipe conveying fourth grade fluid with temperature-dependent viscosities and internal heat generation, *J. Mol. Liq.* 241 (2018) 188–198.
- [57] M.G. Sobamowo, Singular perturbation and differential transform methods to two-dimensional flow of nanofluid in a porous channel with expanding/contracting walls subjected to a uniform transverse magnetic field, *Therm. Sci. Eng. Progress* 4 (2017) 71–84.
- [58] M.G. Sobamowo, On the analysis of laminar flow of viscous fluid through a porous channel with suction/injection at slowly expanding or contracting walls, *J. Comput. Appl. Mech.* 48 (2) (2017) 319–330.
- [59] M.G. Sobamowo, L.O. Jayesimi, Squeezing flow analysis of nanofluid under the effects of magnetic field and slip boundary using Chebyshev spectral collocation method, *Fluid Mech.* 3 (6) (2017).
- [60] M.G. Sobamowo, L.O. Jayesimi, M.A. Waheed, On the Squeezing flow of nanofluid through a porous medium with slip boundary and magnetic field: a comparative study of three approximate analytical methods, *Global J. Eng.* 17 (6) (2017) 61–76.
- [61] M.G. Sobamowo, T.A. Akishilo, A.A. Yinusa, O.A. Adedibu, Nonlinear slip effects on pipe flow and heat transfer of third grade fluid with nonlinear temperature-dependent viscosities and internal heat generation, *Software Eng.* 6 (3) (2018) 69–88.
- [62] A.T. Akinshilo, M.G. Sobamowo, Perturbation solutions for the study of MHD blood as a third grade nanofluid transporting gold nanoparticles through a porous channel, *J. Appl. Computat. Mech.* 3 (2) (2017) 103–113.
- [63] H. Mohsan, M. Marin, E. Rahmat, S.Z. Alamri, Exploration of convective heat transfer and flow characteristics synthesis by Cu-Ag/water hybrid-nanofluids, *Heat Tran. Res.* 49 (18) (2018) 1837–1848.
- [64] R.L. Fosdick, K.R. Rajagopal, Thermodynamics and stability of fluids of third grade, *Procter Soc. Lond.* 339 (1980) 351–377.
- [65] S.N. Majhi, V.R. Nair, Flow of a third grade fluid over a sternosed tubes, *Indian Nat. Sci. Acad.* 60 (3) (1994) 535.
- [66] M. Massoudi, I. Christie, Effects of variable viscosity and viscous dissipation on the flow of a third grade fluid in a pipe, *Int. J. Non Lin. Mech.* 30 (1995) 687.
- [67] M. Yurusoy, Pakdemirli, Approximate analytical solution for the flow of a third grade fluid in a pipe, *Int. J. Non Lin. Mech.* 37 (2002) 187–195.
- [68] K. Vajravelu, J.R. Cannon, D. Rollins, J. Leto, On solutions of some non-Linear differential equations arising in third grade fluid flows, *Int. J. Eng. Sci.* 40 (2002) 1791.
- [69] T. Hayat, S. Nadeem, S. Asghar, A.M. Siddiqui, Fluctuating flow of a third order fluid on a porous plate in a rotating medium, *Int. J. Non Lin. Mech.* 36 (2002) 901–916.
- [70] Y. Muhammet, Similarity solutions to boundary layer equations for third grade non-Newtonian fluid in special channel coordinate system, *J. Theor. Appl. Mech.* 41 (4) (2003) 775–787.
- [71] M. Yurusoy, Flow of a third grade fluid between concentric cylinder, *J. Math. Comput. Appl.* 9 (1) (2004) 11–12.
- [72] M. Pakdemirli, B.S. Yilbas, Entropy generation for a pipe flow of a third grade fluid with Vogel model viscosity, *Int. J. Non Lin. Mech.* 43 (3) (2006) 432–437.
- [73] M. Sajid, R. Mahmood, T. Hayat, Finite element solution for flow of a third grade fluid past a horizontal porous plate with partial slip, *Int. J. Comput. Math. Appl.* 56 (2008) 1236.
- [74] R. Elahi, T. Hayat, F.M. Mahomed, S. Asghar, Effects of slip on the nonlinear flow of the third grade fluid, *J. Nonlinear Anal.* 11 (2010) 139–146.
- [75] O.J. Jayeoba, S.S. Okoya, Approximate analytical solutions for pipe flow of a third grade fluid with variable model of viscosities and heat generation/absorption, *J. Nigerian Math. Soc.* 31 (2012) 207–227.
- [76] S.S. Abbasbandy, T. Hayat, R. Ellahi, S. Asghar, Numerical results of a flow in third grade fluid between two porous walls, *Verlagderzeitschrift fur Naturforschurg* 932 (2008) 51.
- [77] I. Nayak, A.K. Nayak, J. Padhy, Numerical solutions for the flow and heat transfer of a third grade fluid past a porous vertical plate, *J. Adv. Stud. Theor. Phys.* 6 (2012) 615.
- [78] Y.M. Aiyesimi, G.T. Okedayo, O.W. Lawal, Unsteady magneto hydrodynamic (MHD) thin film flow of a third grade fluid with heat transfer and no slip boundary condition down an inclined plane, *Int. J. Phys. Sci.* 8 (19) (2013) 946.
- [79] A.W. Ogunsola, B.A. Peter, Effect of variable viscosity on third grade fluid flow over a radiative surface with Arrhenius reaction, *Int. J. Pure Appl. Sci. Technol.* 22 (1) (2014) 1–2.
- [80] M. Yurusoy, M. Pakdemirli, B.S. Yilbas, Perturbation solution for third grade fluid flowing between parallel plates, *Proc. Inst. Mech. Eng.* 222 (Part C) (2007) 653.
- [81] T. Hayat, H. Nazar, M. Imtiaz, A. Alsaedi, M. Ayub, Axisymmetric squeezing fow of third grade fluid in presence of convective conditions. *Chinese J. Phys.*. Accepted Manuscript.
- [82] W. Zhang, N. Silvi, J. Vlachopoulos, Modelling and experiments of squeezing flow of polymer melts, *Int. Polym. Process. J. Polym. Process. Soc.* (2) (-1995).
- [83] R.J. Grimm, Squeezing flows of polymeric liquids, *AIChE J.* 24 (3) (1978) 427–439. The American Institute of Chemical Engineers.